September 2021

Spatiotemporal Variability of Soil Water δ18O and δ2H Reveals Hydrological Processes in Two Floodplain Soils

Amanda Ceming-Barbato
Louisiana State University and Agricultural and Mechanical College

SPATIOTEMPORAL VARIABILITY OF SOIL WATER $\delta^{18}O$ AND $\delta^{2}H$ REVEALS HYDROLOGICAL PROCESSES IN TWO FLOODPLAIN SOILS

A Thesis

Submitted to the Graduate Faculty of the
Louisiana State University and
Agricultural and Mechanical College
in partial fulfillment of the
requirements for the degree of
Masters of Science

in

The School of Renewable Natural Resources

by
Amanda Ceming-Barbato
B.S., Texas A&M University, 2018
December 2021

ACKNOWLEDGEMENTS

This thesis would not have been possible if it weren't for the continued guidance and counsel of my major advisor Dr. Richard Keim and funding from the Lucius W. Gilbert Foundation. I would also like to thank my committee members Dr. Sammy King and Dr. John Nyman for their feedback and flexibility.

I am grateful for everyone who assisted with lab and field work including Courtney Poirier, Nga Nguyen, Alicia McAlhaney, and Skylar Bueche. Thank you to Dr. Mary Grace Lemon and Savannah Morales for input, assistance, and advice during the early stages of this work. I would also like to pay special regards to Dr. James Nelson for giving me my first lecture on the use of stable isotopes in ecology and for being an invaluable mentor.

Finally, I owe infinite thanks to Asher Spalding for unyielding assistance throughout this study including helping with field and lab work, fixing anything that can be fixed, and encouraging and supporting me through the inevitable ups and downs. Thank you to my cats, Sam, Willow, and Charles for keeping me company and to my parents and brother for continued support.

TABLE OF CONTENTS

ABSTRACT

The movement of water through soil is preferential and heterogeneous. Subsurface interactions between mobile flows and the soil matrix are not uniform and are therefore difficult to predict through time and space. The use of stable isotopes of hydrogen (^{2}H) and oxygen (^{18}O) as conservative tracers of water movement is improving understanding of soil hydrological processes, yet field-scale observations of isotopic variability remain scarce despite implications for identifying dominant hydrologic processes. We sampled two adjacent soils at a ridge-swale topography floodplain forest to determine soil water isotopic variability at a 20 cm depth resolution in soils of differing textures and structures. Soil water isotopic composition measured through direct vapor equilibration varied more in time and space than any mobile source water sampled including throughfall, groundwater, ponded water within the swale, and free water from boreholes. Repeated, replicate soil borings within a rolling 1 m^2 area indicated that soil water isotopic variance by depth was greater in coarser textured ridge soil than in the heavily structured, cohesive clay soil in the swale. Soil water isotopic variance among samples of the same depth and date was not apparently related to soil texture, organic content, or water content. Instead, the timing of soil water isotopic variance seemed to be related to soil structural change as it relates to seasonal hydrologic processes and site topography. Three isotopic mixing models using isotopic composition of throughfall and pre-event soil water were tested to conceptualize the soil water recharge regime at each site. These models represented ideal scenarios of complete bypass flow in which there was no exchange between event water and the soil matrix (test of Two Water Worlds hypothesis), complete replacement by event water (test of complete translatory flow) and conservative mixing between antecedent soil water and event water. At the profile scale, swale soil water was best modeled as rapid replacement by event water and ridge soil water was best modeled as conservative mixing between event water and antecedent soil water. However, variance within the profile of the ridge site showed that conservative mixing was a poor physical model and isotopic variance of soil water was much higher than could be predicted using mean soil water and throughfall isotopic composition alone. These results illustrate that temporal frequency and spatial scale of sampling affect inferences as to what factors control isotopic variability within the critical zone.

INTRODUCTION

Environmental systems are spatially and temporally driven by the influence of water on soil, vegetation, and climate (Rodriguez-Iturbe, 2000). Site hydrology defines vegetative composition, structure, and growth (Rodríguez-González *et al.*, 2010) and can largely control primary productivity in forested wetland systems (Mitsch, 1991). Similarly, soil moisture plays a crucial role in ecological patterns. Extremes in soil moisture can lead to water stressed conditions in vegetation such as decreased photosynthesis and transpiration during periods of low soil moisture and oxygen-limiting conditions during periods of high soil moisture (Rodriguez-Iturbe *et al.*, 2007). Identifying the dominant sources and recharge mechanisms of soil water is essential to understanding system function, predicting ecosystem response to climatic changes, and effectively managing water resources.

Water moves through soils in two major domains: quickly through macropores and slowly through micropores, known as mobile and immobile respectively (Beven and Germann, 1982; Gerke, 2006). Mobile water drains through macropores under the force of gravity whereas immobile water is tightly bound to the soil matrix by capillary forces (Bouma, 1981; Jarvis, 2007; Bowers *et al.*, 2020). Bound water between field capacity and the permanent wilting point is considered plant-available and is preferentially used by plants during photosynthesis and transpiration (Veihmeyer and Hendrickson, 1955; Cassel and Nielsen, 1986). However, recharge into these plant-available water stores and interaction between mobile and tightly bound water are not well understood (Evaristo *et al.*, 2015; Berry *et al.*, 2018).

Stable isotopes of hydrogen (^{2}H) and oxygen (^{18}O) can be used as conservative tracers of water movement to provide valuable information about source, pathway, and process. The use of stable isotope tracers across the field of ecohydrology has led to important findings within the critical zone (Brantley *et al*., 2007): most notably the ecohydrological separation hypothesis (Brooks *et al*., 2010; Evaristo *et al*., 2015; Goldsmith *et al*., 2019; Sprenger *et al*., 2019; Cain *et al*., 2019; Liu *et al*., 2020) also known as the Two Water Worlds hypothesis (McDonnell, 2014), which proposes that plants access water stores isotopically distinct from mobile flows that dominate streamflow. Tracer studies using ^{18}O and ^{2}H support creating more accurate field-scale water models (McDonnell *et al*., 2007; Cain *et al*., 2019) and gaining a greater understanding of solute and contaminant flow (Kung *et al*., 2000). Stable isotopes have also been used to better understand evaporation from soil (Barnes and Allison, 1988), water resource availability and quality (Bowen *et al*., 2011; Bowen and Good, 2015), and source and availability of water to plants (Dawson and Ehleringer, 1991; Evaristo *et al*., 2015; Bowling *et al*., 2017; Berry *et al*, 2018; Allen *et al*., 2019; Sprenger *et al*., 2019).

Recent studies have suggested that subsurface isotopic partitioning and soil water isotopic heterogeneity occurs globally (Jasechko *et al*., 2013; Evaristo *et al*., 2015; Good *et al*., 2015), whereas prior to the widescale application of stable isotopes in soil hydrological field studies, most watershed models considered soil water to be well-mixed and homogenous (Goldmsith *et al*., 2012; Berry *et al*., 2018). Translatory flow, in which incoming water displaces stored water has been cited as the driving mechanism for stimulating the movement of water through soil and mixing water within soil (Hewlett and Hibbert, 1963; Dubbert *et al.*, 2019; Liu *et al*., 2020). However, investigations of soil–water–plant interactions using stable isotopes of hydrogen and oxygen have shown that not all soil water participates in downward flow (Horton and Hawkins, 1965; Sprenger *et al*., 2019) and complete subsurface mixing of soil water cannot

be assumed (Brooks *et al*., 2010; Morales *et al*., 2021). Because tightly bound water does not fully participate in translatory flow, there exists heterogeneity within soil (Evaristo *et al.*, 2015; Sprenger *et al*., 2019). Water that replenishes micropores contributes less to soil water flux, and water in micropores is more tightly bound and is typically older than water in larger pores (Berghuijs and Allen, 2019), making it isotopically distinct from mobile water.

The original source and age of the water in soil may vary not only across the landscape but also vertically within soil. The waters present in soil stores may be derived from precipitation, groundwater, or surface flows depending on the hydrologic regime. Soil physical traits (e.g. texture and structure) largely influence interaction between mobile and bound water in soils by controlling dominant flow processes. Non-equilibrium flow in macropores and variable interactions between mobile and bound water can result in isotopic heterogeneity of soil water (Landon *et al*., 1999). The relationship between mobile and immobile flows is difficult to quantify because water pathways in soil vary based on local and temporal conditions (Jarvis, 2007). Some studies have focused on the soil properties that may contribute to preferential flow dominance or tightly bound immobile water dominance. Berghuijs and Allen (2019) proposed that the law of mass conservation and the transit time distribution of water through soils already explains some variability of soil water isotopic composition. They hypothesize that there is greater isotopic differences between mobile and tightly bound waters in structured soils dominated by preferential flow than in poorly structured soils dominated by translatory flow. Other studies that examined soil physical characteristics found that equilibrium soil water isotopic fractionation depends on soil water tension and is independent of soil texture (Gaj and McDonnell, 2019) meaning soil water isotopic variability cannot be a result of textural and kinetic differences alone.

As work in this field progresses, there is greater emphasis on investigating lateral and vertical characteristics of soil that could result in isotopic heterogeneity (Oerter and Bowen, 2017; Gaj *et al*., 2017; Goldsmith *et al*., 2019). Developing predictive water models for general use requires field level stable isotope data including spatial metrics from differing soils. Nearly–complete, conservative mixing of tightly bound water and mobile water in the soil zone has been proven possible in lab-based studies of disturbed, homogeneous soils (Bowers *et al*., 2020). The complete equilibration of pore waters when structure is disturbed adds supportive evidence to the claim that subsurface stores are not inherently ‘disjunct’ (Sprenger *et al*., 2019) but rather that water flows heterogeneously through them (Berghuijs and Allen, 2019; Radolinski *et al*., 2021). In heavily aggregated soils such as clays, total equilibration of pore waters may take much longer than in homogenous sandy loam soils (Bowers *et al*., 2020). In fact, Morales *et al*., (2021) found that vertic soils did not fully equilibrate even after 31 days of flooding.

Soil water isotopic variability is likely a culmination of soil physical traits as well as less understood kinetic processes. The isotopic variability of tightly bound water as compared to mobile water cannot be explained by fractionation effects of evaporation alone (Goldsmith *et al*., 2012). Furthermore, the increased contact with soil solid surfaces complicates stable isotope interactions through less understood fractionation effects (Oerter *et al*., 2014; Lin and Horita, 2016; Gaj *et al*., 2017).

Isotopic variability exists at numerous scales and has implications for our understanding of hydrologic processes at the watershed level. The assumption that soil water is merely derivative of dominant source water (e.g. throughfall) isotopic composition is conceptually based

on an oversimplification because sources are themselves variable (Goldsmith *et al*., 2019). Constraining variability in source water as it relates to recharge of soil water is essential to acquiring data useful for addressing the degree of interaction between mobile and immobile waters. Although lab-based soil water isotope studies can provide valuable insight on flow regime (Horton and Hawkins, 1965; Gazis and Feng, 2004), mixing of mobile and immobile waters (Bowers *et al*., 2020; Radolinski, 2021), and interactions in the critical zone (Barnes and Allison, 1988; Gazis and Feng, 2003; McDonnell, 2014; von Freyberg *et al*., 2020) these studies often offer limited insight to field-scale processes in natural systems where multiple sources and processes overlap.

Water sources to floodplain soils are variable and hydrological interactions are often complex. Floodplains may receive water from precipitation, overbank flooding, shallow groundwater, and exchange with the hyporheic zone (Mertes, 1997; Bendix and Hupp, 2000; Woessner, 2000). However, implementation of flood control structures and conversion of forests to agricultural use has reduced hydrological connectivity of floodplain ecosystems (King *et al*., 2009). Productivity of tree species in floodplain forests is related to soil moisture availability and overall hydrologic regime (Gee *et al*., 2014). Limited hydrological connectivity and reduced water source can impart stress on vegetation even in floodplain wetlands characterized by annual water excess (Sun *et al*., 2002). It is therefore important to determine source water interactions within floodplain soils for management of these often-degraded environments.

This study aims to understand the spatial (lateral and with depth) and temporal variability of soil water within two adjacent but texturally distinct soils in a floodplain, by monitoring isotopic composition of water sources and soil moisture. We present three narrow objectives:

1) Determine the isotopic variability of soil waters in two adjacent soils of differing texture and structure.
2) Determine sources and mechanisms of soil water recharge.
3) Constrain variables affecting soil water isotopic variability.

METHODS

2.1. Overview

This study employed frequent soil and source water sampling methods to capture detailed changes in soil water over time. Replicated and repeated sampling of soils within rolling 1^2 m patches were used to estimate the spatiotemporal variability of soil water isotopic composition. Soil samples were used to determine water content, isotopic composition of soil water, particle size distribution, and organic matter content. Free water was collected from boreholes for isotopic analysis whenever present. We sampled two adjacent sites at one study area from January to December of 2020. The sample area spanned approximately 15,000 m^2. Groundwater level was recorded continuously in one shallow monitoring well at each site and water samples were routinely collected. Roving throughfall collectors were used at each sample location and surface water and some samples of large storm direct precipitation were also collected. Stable isotopes of hydrogen and oxygen (^2H and ^{18}O) were used as conservative tracers of sources of water within forest soil from several candidate contributing source waters (throughfall, groundwater, and surface water).

2.2. Site Description

This study was conducted at Louisiana State University Agricultural Center Central Research Station (informally known as Ben Hur Forest) approximately 3 km south of Louisiana State University (Figure 1). The total area of this forest is approximately 0.6 km^2. The north, south, and west sides are bound by residential neighborhoods and the east side is open farm land.

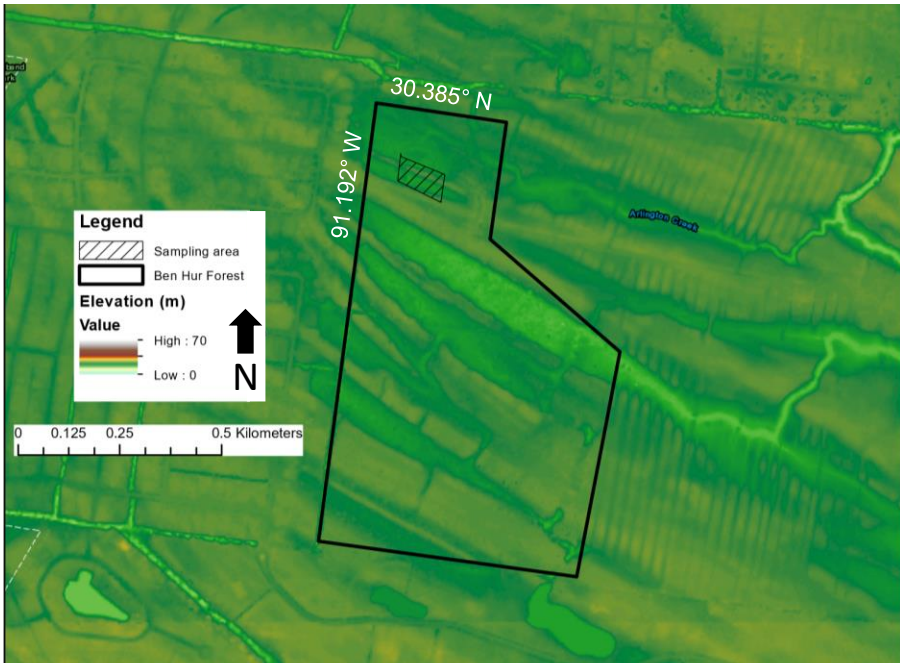

Figure 1. Map of study area.

Ben Hur Forest is a bottomland hardwood forest in a humid subtropical climate. Dominant tree species present at Ben Hur Forest include American elm (*Ulmus americana*), cherrybark oak (*Quercus pagoda*), sweetgum (*Liquidambar styraciflua*), cow oak (*Quercus michauxii*), and sugarberry (*Celtis laevigata*) along the ridges (Reid, 2019) and baldcypress (*Taxodium*

distichum), water tupelo (*Nyssa aquatica*), Nuttall oak (*Quercus texana*), water hickory (*Carya aquatica*), and Drummond red maple (*Acer rubrum* var. *drummondii*) in the swales (Moerschbaecher *et al*., 2016). The mean annual precipitation in this region is approximately 178 cm (NOAA, 2021a).

Located less than 3 km east of the Mississippi River, this forest was once periodically flooded by the Mississippi River before the construction of levees beginning prior to 1800 (U.S. Army Corps of Engineers, 2021). Geomorphically, the sample area is ridge-swale topography formed through Mississippi River meandering. The ridge surface is 1.24 m above the swale, making the ridge approximately 6.9 m above sea level. The surface of the swale is graded westward and surface water likely drains west into a ditch that borders the forest. This topography means that two differing soils are juxtaposed but subject to the same meteoric events.

The soils are typical of alluvial ridge-swale sequences, with coarser-textured sediments composing the ridge, but there is a mantle of clayey deposition over the ridge indicating deposition of sediments in slow-moving flood waters following the initial formation of the ridge-swale sequence. The soil on the ridge (Thibaut) is a clayey over loamy, smectitic, hyperthermic Vertic Epiaquept (Soil Survey Staff, 2019). There is a greater concentration of clay near the surface and a textural discontinuity from silt to very fine sand at 70 cm. The structure of the ridge soil is blocky within the upper meter but becomes massive at depths greater than 1 m with iron concretions throughout. The soil in the swale (Schriever) is a very fine, smectitic, hyperthermic Chromic Epiaquert (Soil Survey Staff, 2019). It is a poorly drained clay soil with a blocky structure.

2.2.1. Soil particle size analysis

Particle size analysis was conducted by depth class (20 cm resolution) on two profiles for each soil series using a laser diffraction particle size analyzer (S3500, Microtrac, Montgomeryville, PA, USA). For each sample, 30 g air-dried and ground soil was added to a beaker with 150 mL deionized water to rehydrate the samples. Large organic matter was removed by passing the soil through a 2 mm sieve. Small organic matter was digested by adding 30% H_2O_2 in 5 mL increments until excessive frothing ceased (Klute, 1986) and color changed significantly. The soil samples were air dried and then shaken in a 22% sodium hexametaphosphate solution to deflocculate aggregates. Due to the heavy clay content of the soils, analyses assumed irregularly shaped particles, an absorption coefficient to account for nearly transparent particles, and a refractive index of 1.54 (Özer *et al*., 2010; Jena *et al*., 2013).

The particle size of both ridge and swale soils varied by depth (Figure 2). Using the Wentworth (1922) scale size fraction classification, the ridge soil texture was approximately 39% sand, 44% silt, and 17% clay, but with more clay at the surface and less at depth. Swale soil texture was approximately 6% sand, 65% silt, and 29% clay. Below 70 cm in ridge soils, the grain sizes shifted from silt to very fine sand (peaks within the range of 0.062 to 0.125 mm). There was a larger proportion of clay-sized grains in swale soil consistent with depth as compared to ridge soil. Swale soils were considered to be very fine silt (< 0.0078 mm) at depths of 70, 90, and 110 cm. The median grain size of swale soil shifted to medium silt (< 0.0156 mm) at 150 cm depth and all depths show a small (< 1%) probability density percentage of sand-sized grains. Clay-sized particles are likely underrepresented in the data due to underestimation of fine grain sizes in silty soils by laser diffraction (Beuselinck *et al*., 1998).

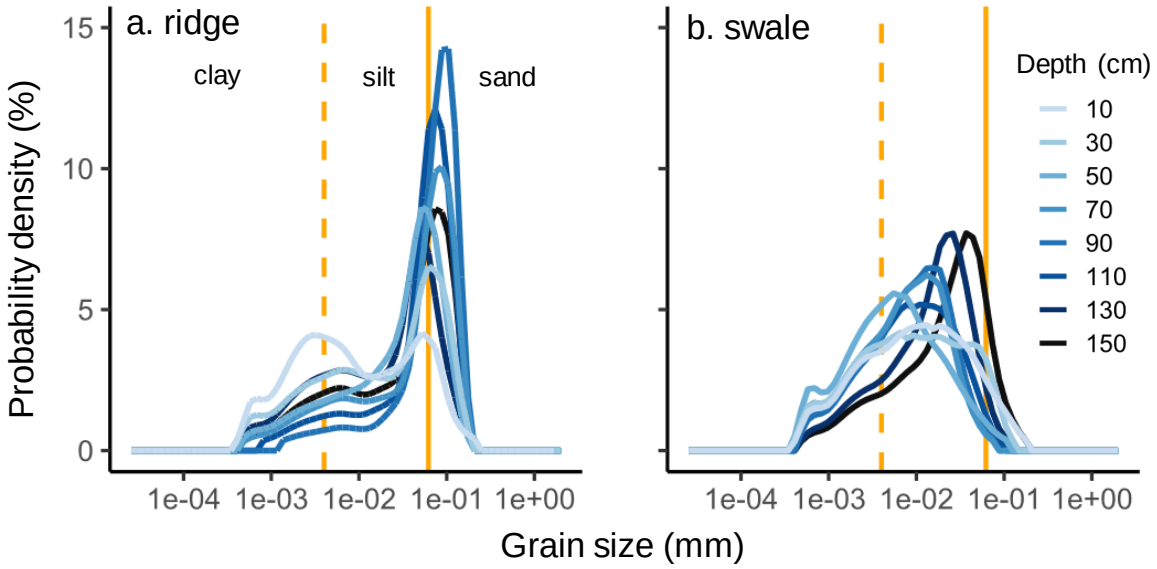

Figure 2. Particle size distributions for the (a) ridge and (b) swale soils by depth.

2.2.2. Organic matter

Organic matter (OM) content was determined for each soil sample using the loss-on-ignition (LOI) method. Soil was dried at 105 ºC to remove hydroscopic water, ground in a soil mill, placed into an aluminum tin, and weighed using a balance with a resolution of 0.001 g. The soil was then ignited in a muffle furnace for two hours at 550 °C. This exposure time was chosen to limit variation in LOI based on variations of sample weight (Heiri *et al*., 2001). The percent mass loss in the post burn samples was used to determine the OM content. There is an upwards bias of LOI in clay soils created by structural water loss at temperatures above 375ºC (Ball, 1964). This bias could account for 4-6% of weight loss from LOI in clay soils (Dean, 1974, Ball, 1964) but the actual amount is unknown. Therefore, OM for this study is reported as OM_{LOI} (%).

Soil OM_{LOI} decreased with depth at both sites (Figure 3). OM_{LOI} was greatest at a depth of 10 cm. Swale soil was overall more organic than ridge soil. Mean OM_{LOI} of ridge soil across all depths was 4.2% and the mean OM_{LOI} of the swale soil across all depths was 7.2%. Estimates of OM_{LOI} content vary depending on clay content, therefore the actual OM content in either soil may be up to 6% less than reported.

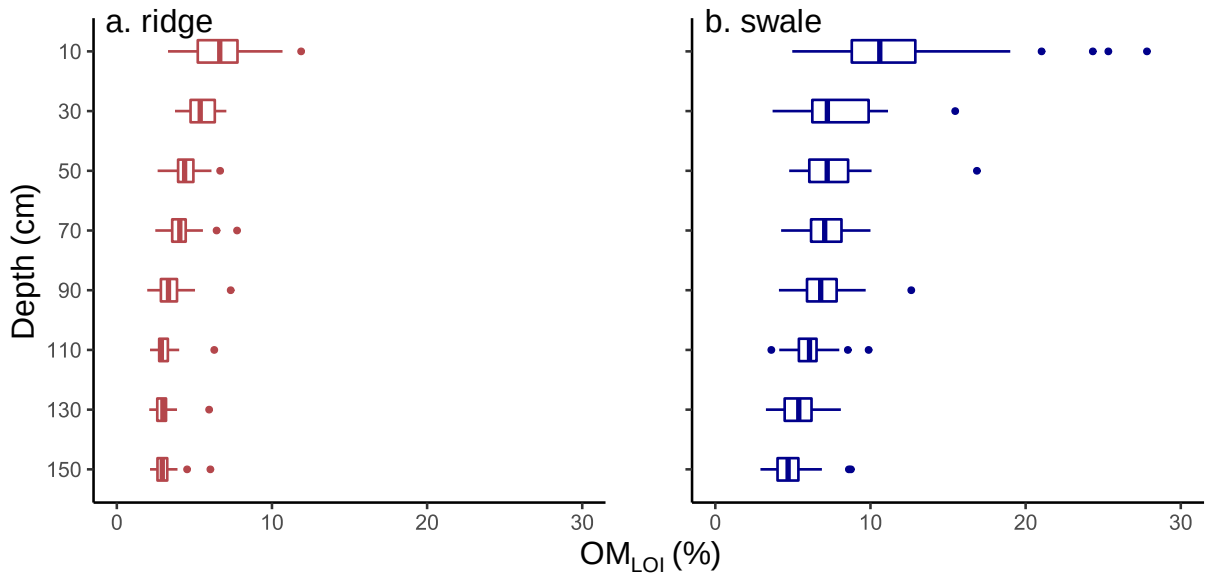

Figure 3. Organic matter by loss on ignition for (a) ridge and (b) swale soils by depth. The box represents the interquartile range, the vertical bar represents the median, and the points represent outliers.

2.3. Sample Collection

2.3.1. Groundwater wells

Shallow groundwater monitoring wells were established at each site (ridge and swale). The swale well reached 2.5 meters below ground surface and the ridge well reached 2.2 meters below ground surface. The elevation of the ground at the ridge well site was 1.2 m higher than the ground at the swale wells site, determined using an optical level. The PVC well casings were vented and screened throughout their length. A non-vented pressure transducer (Hobo U20-001-01, Onset Computer, Bourne, MA, USA) was installed at the bottom of each well to continuously record pressure. Water level in the wells was calculated after correction for atmospheric pressure which was recorded by another pressure transducer located above ground surface at the study area. Any gaps in atmospheric pressure data were reconciled using data from Baton Rouge Metro Airport (NOAA, 2021b).

Groundwater samples were collected from both wells on a bi-weekly basis. Wells were bailed then allowed to refill and a sample was taken for stable isotope analysis in a zero-headspace 20 mL glass scintillation vial.

2.3.2. Throughfall and precipitation

Throughfall was collected at each sample site using covered plastic bottles standing 20 cm above the ground fitted with a funnel. A ping pong ball was placed in each funnel to cover the opening and reduce evaporation between rain events and collections. Each site had 5 roving samplers which were relocated to the next soil sampling location (approximately 5 m away) after each collection. This roving method was used to collect the throughfall isotopic composition that would be informing the next soil sampling location. Multiple throughfall collectors were used to capture intra- and inter-storm variability (Keim *et al*., 2005; Hsueh *et al*., 2016) that can contribute to variability in soil structure and water fluxes (Metzger *et al*., 2017). Samples of

throughfall from each collector were taken and stored in a zero-headspace 20 mL glass scintillation vial for isotope analysis.

A Louisiana State University Agriclimatic Information System rain gauge located approximately 2.5 km away from the study area was monitored for rain events. Data from this rain gauge was also used to inform precipitation amount for water budgets and isotope modeling instead of the roving throughfall collectors. A constant 20% interception loss was chosen to inform throughfall amount (Pataki and Oren, 2003; Bryant *et al*., 2005; Yue *et al*., 2021) because of problems associated with undercatch by the roving throughfall collectors. Direct precipitation for selected large storms was captured in one 5-gallon Nalgene bottle fitted with a funnel and ping pong ball in the open field bordering the east side of the sample site. The precipitation was measured, recorded, and collected the same way as throughfall samples. The isotopic composition of the precipitation was used to inform the isotopic accuracy of the roving throughfall collection method but was otherwise not used for soil water analyses.

2.3.3. Surface water and free water

Samples of surface water were collected whenever present during biweekly sampling and stored in zero-headspace 20 mL glass scintillation vials for analysis of isotopic composition. Surface water was generally present in low lying areas within the swale. Similarly, any free, gravitational water within soil boreholes was collected. These samples include waters visibly flowing from macropores (mainly root channels) and water infiltrating into the borehole from no distinct source (i.e. free, gravitational water).

2.3.4. Soil

Soil samples were collected during fifteen sampling dates spanning January through December of 2020. At each soil sampling event, ridge and swale soil samples were collected in replicated boreholes, at 20-cm depth increments down to 1.5 meters (excluding the upper 10 cm) using a manual soil auger. Replicate boreholes were within 1 m^2. The soil collected was temporarily stored in Ziploc bags for transport from the field. Each sample collection location was approximately 5 meters west of the previous location, along the respective ridge and swale, allowing for a buffer of undisturbed soil between sampling locations to prevent hydrologic influence from previous soil excavations. Ridge and swale sampling events were parallel to each other to ensure that all atmospheric parameters and soil hydrologic differences were more comparable. When the swale was flooded, soil sampling occurred in low lying regions near the edge of the ponded surface water, occasionally in episaturated conditions. Swale soil samples were taken in the same manner during unsaturated surface conditions for methodological consistency.

2.4. Analysis

2.4.1. Water content

The fresh weight of each sample was measured for moisture content prior to stable isotope analysis. Following analysis of soil water isotopic composition, the soils were removed from the vapor equilibration bags and baked at 105 ºC for a minimum of 72 hours. The oven-dry mass of the samples were then measured and used to calculate water content.

2.4.2. Stable isotope analysis

Stable isotope analysis was conducted in liquid phase for free water sources and in vapor phase for bound water within soils.

2.4.2.1. Liquid water

Isotopic analysis of waters was conducted using off-axis integrated cavity output spectroscopy (OA-ICOS) (LGR-IWA-45-EP, Los Gatos Research, Los Gatos, CA, USA). All measurements of δ^2H and $\delta^{18}O$ are relative to Vienna Standard Mean Oceanic Water (VSMOW). Deuterium and oxygen-18 isotope values are expressed in per mille notation calculated as δ^2H or $\delta^{18}O$ (‰) $= \left(\left(\frac{R_{sample}}{R_{standard}}\right) - 1\right) \cdot 1000$ where R is the ratio of ^{18}O to ^{16}O or ^2H to H in the sample or VSMOW standard.

All liquid water samples were processed for isotopic analysis in the same manner. Suspended sediment and debris within the water samples were filtered using a 45-micron syringe filter prior to liquid water isotope analysis. Three in-house reference standards were used as precision controls during isotopic analysis. The batch method was used, alternating between sets of samples and sets of standards throughout the analyses (Arggarwal *et al*., 2009). An internal control of known isotopic composition was also included as a sample twice to account for instrumental drift and to estimate precision. Each standard and sample were injected into the vacuum chamber eight times and the first four injections were discarded in effort to reduce memory effects (Penna *et al*., 2012). LGR post-analysis software was used for quality control to identify deviation of controls greater than 0.2 ‰ for ^{18}O and 0.6‰ for ^2H as well as any instrument error such as temperature changes, pressure changes, and injected volume deviation).

2.4.2.2. Direct vapor equilibration

Soil water isotopic composition was determined using the direct vapor equilibration method (Wassenaar *et al*., 2008) to target bulk (plant available) water stores within the soil (Millar *et al*., 2019). Once fresh mass was recorded for each sample, the soil samples were transferred into leak-tight, heat sealed 10 L volume, side-gusseted bags (PBFY Flexible Packaging, Portland, TN, USA; Grahler *et al*., 2018), pumped with room air, and placed in the same temperature-monitored room as the laser isotope analyzer (LGR IWA-45-EP) for at least 72 hours to allow for complete equilibration of soil water within the bags. Three sets of standards and internal controls were prepped on the same day as the samples by placing 4 mLs of liquid standard into the heat-sealed bags, treating, prepping, and storing them identically to the soil samples (Hendry *et al*., 2015). Vapor standards were analyzed at the beginning, middle, and end of each batch and an internal control was analyzed between the standard sets to check for machine drift. Recording thermometers logged the temperature of the room at 15 min intervals (Hobo U20-001-01, Onset Computer, Bourne, MA, USA). The average temperature over the equilibration period was used to define the temperature-dependent fractionation coefficient of liquid water to vapor (α) (Majoube, 1971). To analyze samples, the bags were punctured with an 18-gauge needle attached to an intake line that continuously fed the vapor from the headspace into the isotope analyzer. Parafilm was used to create a seal between the puncture and the needle to reduce leakage of lab air into the sample stream (Lemon, 2020). We aimed for 4 min of continuous vapor flow from each bag followed by one minute of room air between samples which served as a quality control to flush moist air from the intake line and chamber. Only the most saturated portion of the 4 min interval was used to determine the mean isotopic composition. The first minute of the vapor intake was excluded to prevent influence from room air and the last minute was excluded to reduce the possibility of liquid water on the inside of the bag being measured as equilibrium vapor nearing deflation (Lemon, 2020). A quality control threshold of 90% or greater relative humidity in the sample stream was used to ensure closed-

system equilibration of soil water and ambient air within the equilibrium bags. Any bags that were found to be incompletely sealed, leaky, or have low H_2O concentration indicating potential non-equilibrium (kinetic fractionation) conditions were discarded.

All soil water isotope values were converted to their liquid equivalent using the fractionation coefficient (α) determined by the mean room temperature during the equilibration period. A calibration curve was created using the standards known liquid values and samples were corrected to this curve. Experimental precision was calculated as 1.9‰ for δ^2H and 0.6‰ for $\delta^{18}O$, equal to the standard deviation from known isotopic composition of the last standard set from each sample run.

2.4.3. Bulk density

Soil bulk density was determined to estimate soil porosity. Soil water content was determined by multiplying gravimetric water content by the average bulk density at each site to obtain volumetric water content which was used for modeling. The bulk density of ridge soil was determined incrementally to a depth of 100 cm using a hammer core. The soil cores were dried at 105º C for 72 hours until constant weight. The weights of the hammer core cylinders were averaged and subtracted from the dry soil weight. Dry bulk density was calculated at each depth and averaged for the ridge site. A different field method was used for the swale soil because highly saturated soil conditions made accurate use of the hammer core more difficult.

Data from Shockey *et al*., (2021) who reported precise measures of soil physical parameters from a similar swale 15 km away, were used to determine the bulk density of swale soil. The values reported by Shockey *et al*., (2021) were compared to field data acquired at the swale site. The entire mass of soil removed at each depth was conserved and the volume of the sample was calculated as the circular area of the auger hole multiplied by the sample depth. A subsample from each depth increment was weighed, dried at 105º C until constant weight, and the dry mass was proportioned to the total sample mass it represented. The overall average resulted in a bulk density of 1.1 g/cm^3 which is comparable to the 1.04 g/cm^3 average reported by Shockey *et al*., (2021). A value of 1.1 g/cm^3 was used for depths below 10 cm, and a value of 0.8 g/cm^3 was used for soil at 10 cm depth due to saturated conditions and surface ponding.

2.4.4. Water budget and soil water model

A soil water budget was created to predict water content during each sampling based on soil water content in the prior sampling, throughfall, and evapotranspiration. Simplified assumptions were that 1) all throughfall infiltrates into the soil and there is no surface runoff or deep drainage; 2) ponded water within the swale has no effect on water content. The water budget was

$$VWC_t = VWC_{t-1} + TF - ET \quad (1)$$

where VWC is volumetric soil water content at sample period *t*, TF is throughfall, and ET is evapotranspiration.

The mean volumetric water content at each site (ridge and swale) for each sample date was computed. Soil water content was converted from volumetric (mL) to linear units (mm) by multiplying by the entire sample depth (1500 mm). The amount of throughfall between sampling events (mm) was calculated using the sum of rainfall between events and the assumption of constant 20% canopy interception loss. Evapotranspiration (ET) was estimated using data from Moderate Resolution Imaging Spectroradiometer (MODIS) and Global Land Data Assimilation

Systems (GLDAS) datasets in the Penman-Monteith-Leuning (PML-V2) model (Monteith, 1964; Leuning *et al*., 2008; Zhang *et al*., 2019). The PML-V2 estimates of transpiration and direct evaporation from the soil surface were combined. The data source was an 8-day average at a 500 m resolution (Zhang *et al*., 2019). The 8-day average was expanded to a daily average to calculate the average sum of ET between sample periods in millimeters. All differences between ridge and swale soil water predictions are attributed to differences in antecedent soil water content (VWC_{t-1}) since predictions of both sites used the same quantity of evaporation and throughfall.

2.4.5. Isotope models

Three models of soil water isotopic composition were created. The main model assumed conservative mixing between throughfall and pre-event water as:

$$\delta^2H_{mix} \text{ or } \delta^{18}O_{mix} = \frac{(\delta_{soil} \cdot VWC_{soil}) + (\delta_{TF} \cdot precip_{TF})}{wc_{soil} + precip_{TF}} \quad (2)$$

where δ_{soil} is the mean δ^2H or $\delta^{18}O$ of previous soil water sampling, VWC_{soil} is the average soil water content (mm) of previous soil water sampling, δ_{TF} is the is the volume-weighted mean δ^2H or $\delta^{18}O$ of the throughfall collected for the period preceding the sampling date, and $precip_{TF}$ is the amount of throughfall between sampling events (mm) derived from rain gauge data with the assumption of constant 20% interception loss. The conservative mixing model was compared with two null models: Replacement (all soil water the same as throughfall) and No Exchange (throughfall had no effect on soil water isotopic composition).

2.4.6. Local meteoric throughfall line and line-conditioned excess

A local meteoric throughfall line (LMTL) was constructed from the volume weighted mean isotopic composition for each collection date of throughfall. The LMTL informed the calculation of line-conditioned (lc) excess, in which $lc\text{-}excess = \delta^2H - a \cdot \delta^{18}O - b$ where a and b are the slope and intercept of the LMTL respectively (Landwehr and Coplen, 2004). Lc-excess characterizes processes that result in isotopic deviation from presumed source, such as evaporation (negative lc-excess) or distillation (positive lc-excess).

RESULTS

There was a seasonal trend of elevated groundwater level throughout the winter and spring, declining water level during the summer, and much lower water level during the fall before winter wet up (Figure 4). Leaf out in mid-March coincided with decreased groundwater level within the ridge but not the swale, where it remained above the surface until mid-June. Following this initial groundwater recession within the swale, rain events caused intermittent ponding at the surface. Ridge and swale groundwater level responded similarly to rainfall events during the winter and spring. There was a greater effect of late summer rain events on groundwater level in the swale than in the ridge. Timing of wet-up between sites was similar, but recession from storm events was generally slower in the ridge than in the swale. Uncertainty in water level measurements increased during periods of drought, when the water level dropped below the lower extent of wells. There was evidence of subsurface lateral exchange between sites: during periods of high water within the swale there was a gradient from the swale into the ridge, but during periods of drawdown, the gradient was reversed and flow was likely lateral from the ridge into the swale. There was a gradient from the nearly-saturated swale into the ridge during winter wet up.

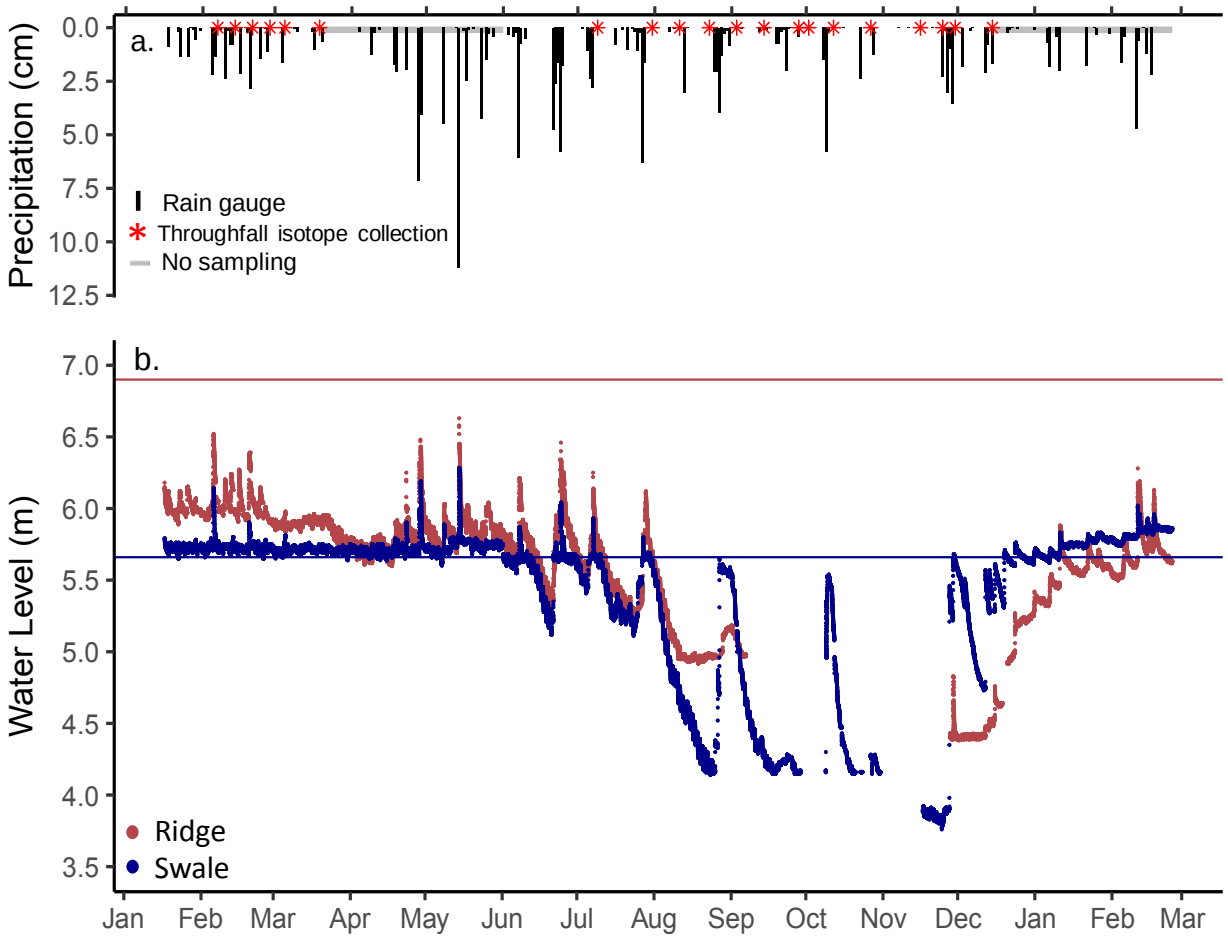

Figure 4. (a) Time series of daily precipitation summary from local rain gauge. (b) Time series of groundwater level at the ridge and swale sites. The horizontal blue line represents ground surface of the swale site and the horizontal red line represents ground surface of the ridge site.

Soil water content varied through time similarly between sites (Figure 5). Shallow soil (within the upper 70 cm) volumetric water content in the swale was always greater than shallow soil volumetric water content on the ridge (Figure 6 a and b). Soil moisture responded to seasonal recession of groundwater in August at both sites. Ridge soils remained drier than swale soils through samplings in the summer and fall. Swale soil water content decreased with depth (Figure 6 b), with the exception of only two sample periods (Feb 28 and Oct 15). At samplings during the winter and spring, ridge soil water content was consistent with depth. At samplings during the summer following groundwater recession, ridge soil water content decreased with depth until approximately 130 cm where soil water content slightly increased. Soil water content in the swale soils became more consistent with depth following groundwater recession in August.

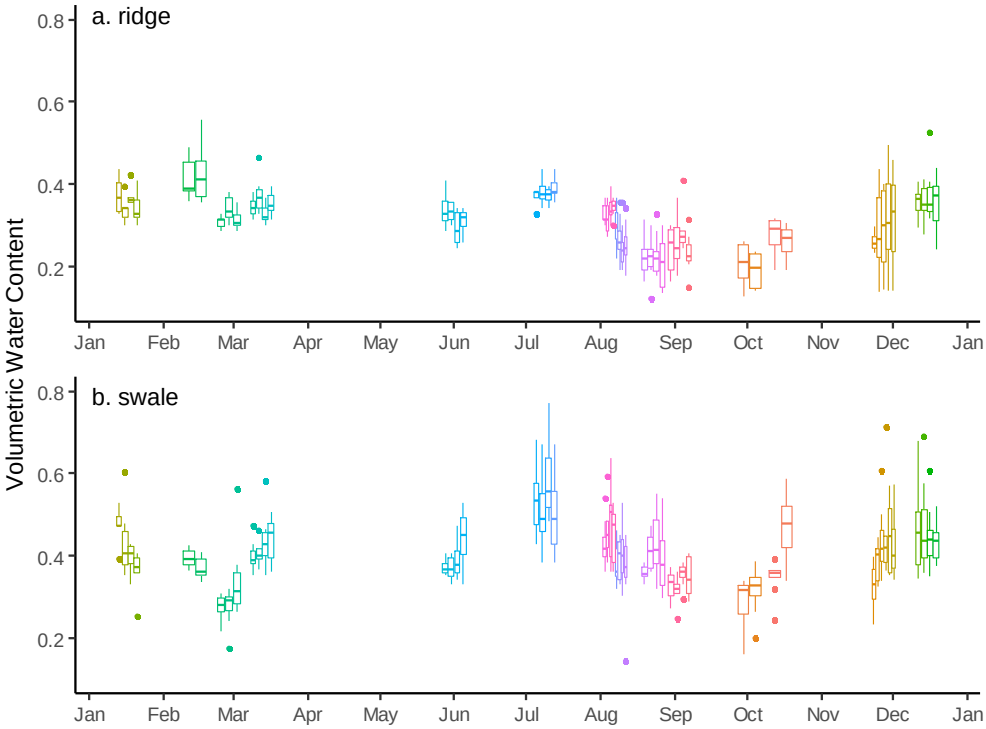

Figure 5. Volumetric soil water content of each borehole extracted at the (a) ridge and (b) swale sites through time. Each box represents the interquartile range, the horizontal bar represents the median, and the points represent outliers.

Soil water content was more predictable in ridge soils ($R^2 = 0.67$) than swale soils ($R^2 = 0.18$) with predictions based off a simple water balance (Figure 7). The sum of the deviation from prediction was 237 mm in the ridge and 192 mm in the swale, meaning predictions were more likely to overestimate soil water content at both sites. Overall, the mean deviation from prediction was 15 mm in the swale and 18 mm in the ridge. Deviations between predicted and observed water content did not always trend in the same direction between sites. For example, the first prediction (Feb 14) underestimated water content by 21 mm in the ridge and overestimated water content by 125 mm in the swale. The runoff ratio was approximately 22% in the ridge and 17% in the swale, calculated as the sum of deviation from prediction divided by the total rainfall and neglecting any run-on into the swale.

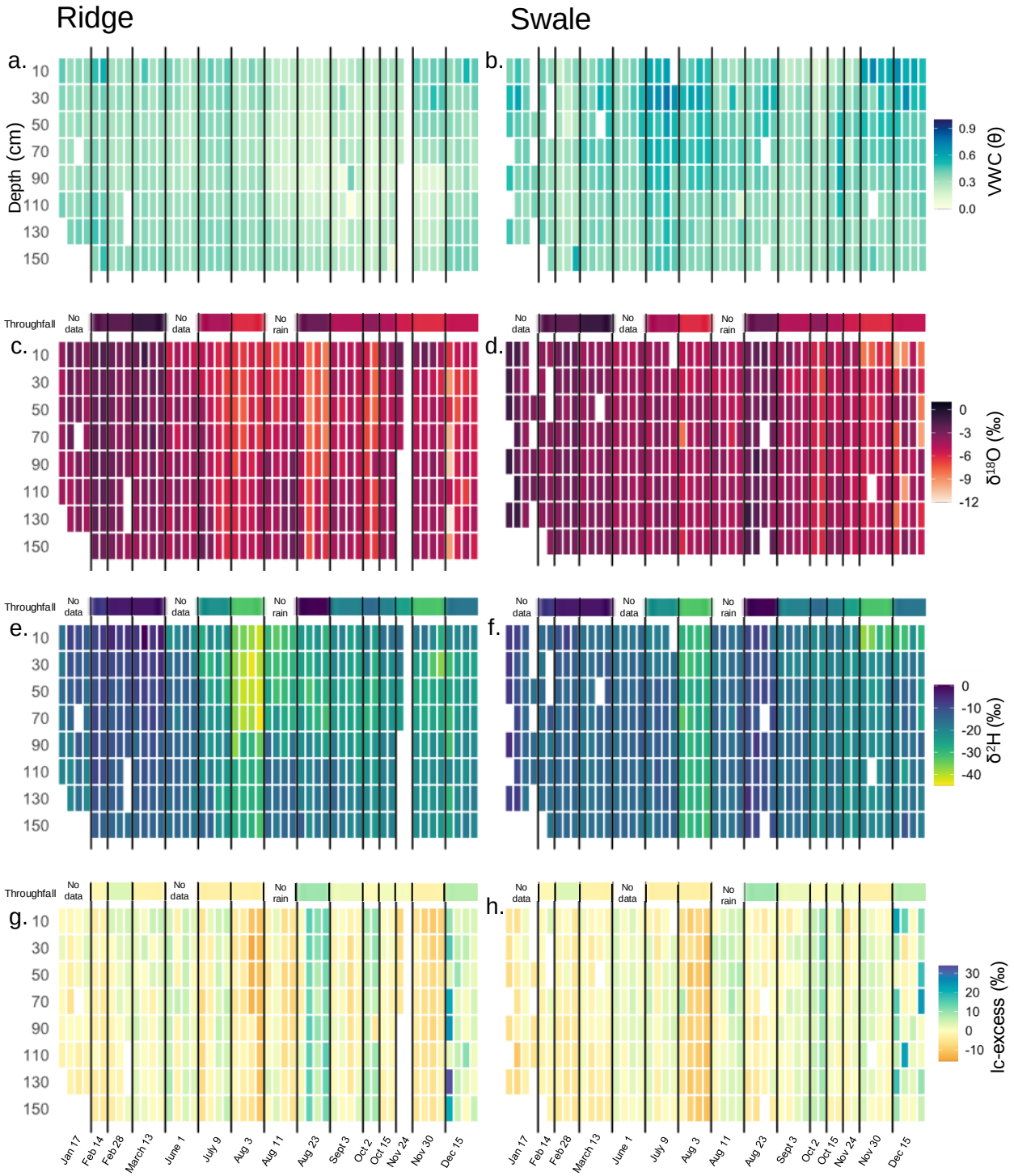

Figure 6. (a, b) volumetric water content, (c, d) $\delta^{18}O$, (e, f) $\delta^{2}H$, and (g, h) line-conditioned excess paired with respective volume-weighted throughfall isotopic composition informing each soil sampling above for (left) ridge and (right) swale sites. Columns represent each hole excavated throughout the full period of study.

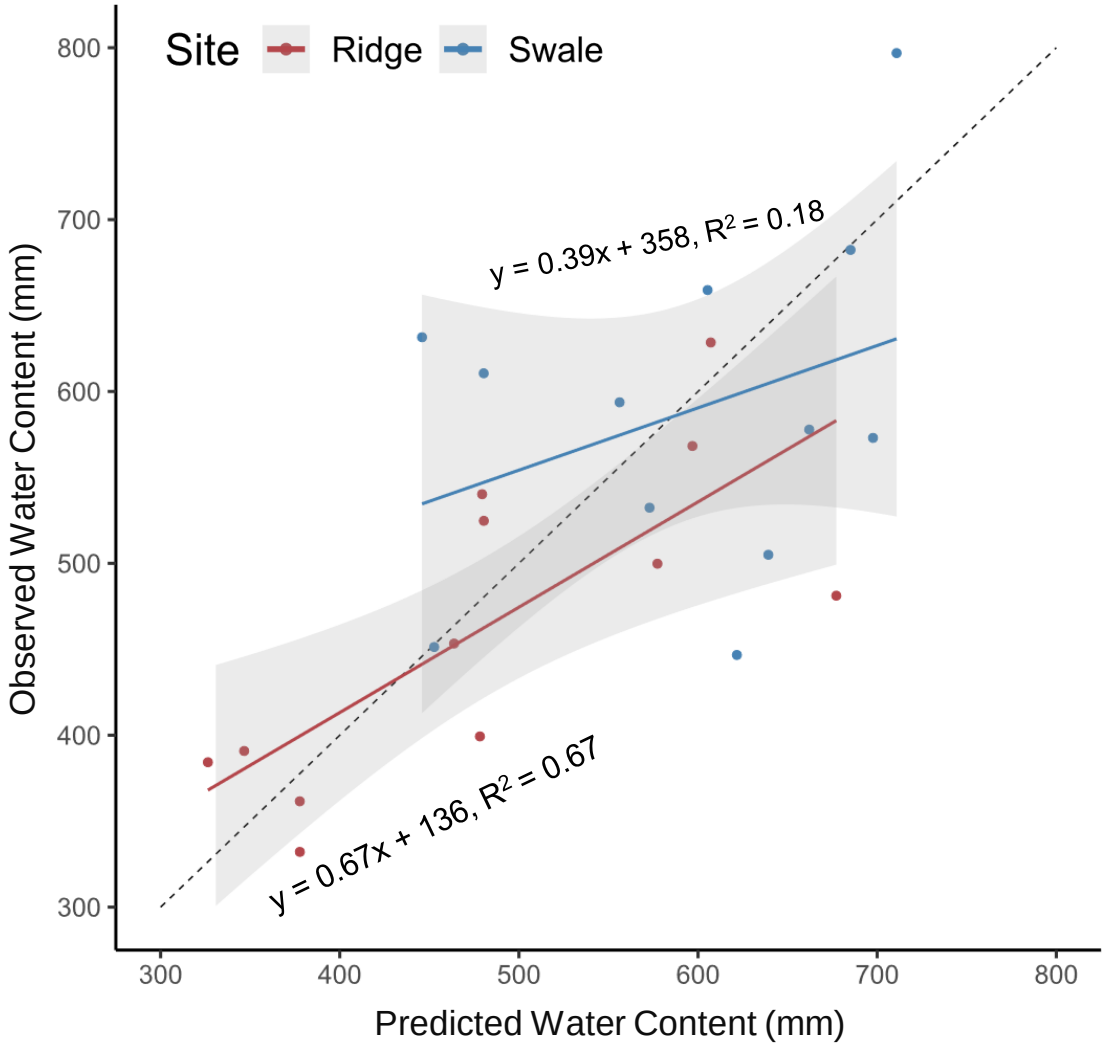

Figure 7. Linear mixing model of soil water content including predictions for ridge and swale sites. Predictions are a function of observed antecedent water content and date. Grey shaded region represents the 95% confidence interval of each model. Dashed line represents 1:1 relationship of predicted to observed water content.

There was no apparent difference in the volume or the isotopic composition of the throughfall collected between the ridge and swale sites, so all data were combined for construction of the local meteoric throughfall line (LMTL) (Figure 8). Approximately 54 cm of throughfall was collected throughout the duration of this study. The volume-weighted LMTL was $\delta^2H = 5.75\ (\delta^{18}O) + 6$ as informed by the volume-weighted average isotopic composition of 19 storms (162 total throughfall samples). Throughfall isotopic composition was less variable intra-event than inter-event with the exception of throughfall collected on Feb 28. There was no discernable relationship between throughfall amount and isotopic composition or season.

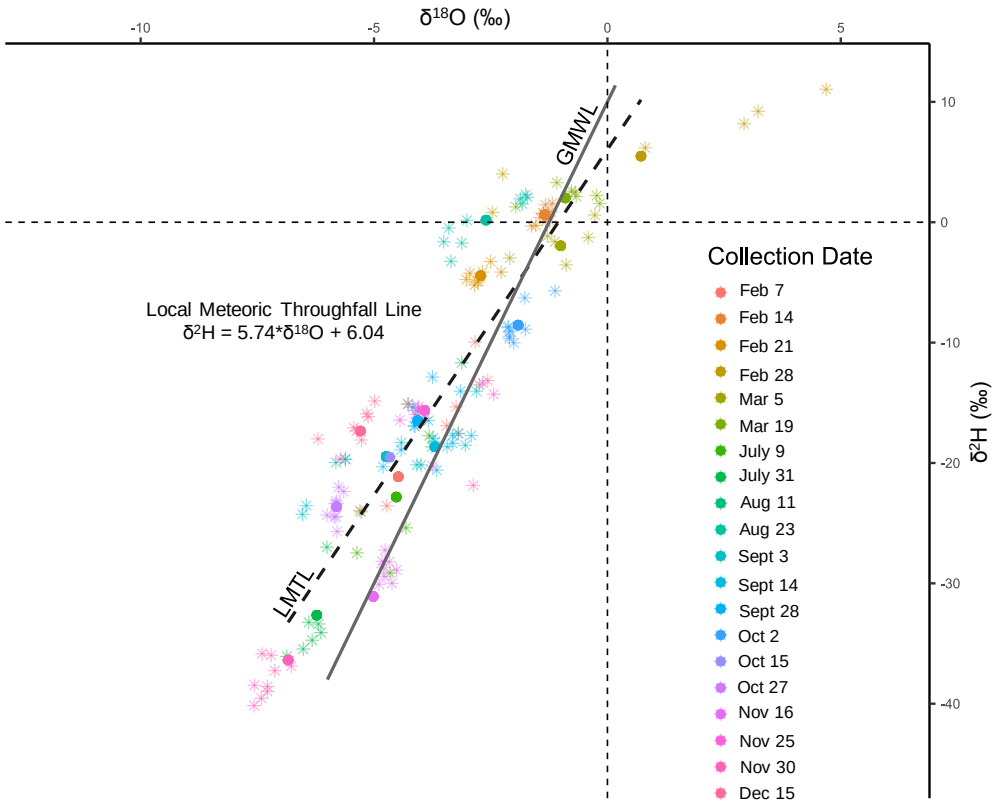

Figure 8. Weighted Local Meteoric Throughfall Line (LMTL) compared to the Global Meteoric Water Line (GMWL) in dual isotope space. Points represent the weighted average isotopic composition of each rain collection and asterisks represent the isotopic composition of individual throughfall collectors.

Isotopic composition of soil waters varied between the ridge and swale sites and through time (Figure 6 c-h). The overall mean isotopic composition of soil water was -4.7‰ for $\delta^{18}O$ and -20‰ for $\delta^{2}H$ in the ridge, and -4.1‰ for $\delta^{18}O$ and -18‰ for $\delta^{2}H$ in the swale. There was a wider range of $\delta^{18}O$ and $\delta^{2}H$ in ridge soils than in swale soils (Table 1 and Figure 9). Ridge soil water was more depleted in $\delta^{2}H$ on Aug 3 than prior throughfall was and remained depleted for longer than swale soil water (Figure 6 e). The isotopic composition of swale soil water was more consistent through time and generally more enriched in both $\delta^{18}O$ and $\delta^{2}H$ as compared to the isotopic composition of ridge soil water. Lc-excess was comparable between sites from January through early August. The mean lc-excess of all soil samples in the ridge was 0.1‰ greater than the mean lc-excess of all soil samples in the swale. The sites differed most in lc-excess during samplings in the fall and early winter, when soils were driest. For example, the mean difference in soil water lc-excess between sites was 11‰ (mean lc-excess of ridge soils was +9‰ and mean lc-excess of swale soils was -2‰) and swale soil water sampled on August 23 was 2.4‰ more enriched in $\delta^{18}O$ and 12‰ more enriched in $\delta^{2}H$ than ridge soil water.

Table 1. Relationship between δ^2H and $\delta^{18}O$, range of δ^2H and $\delta^{18}O$, and (*n*) the number of samples collected for each sampled water source.

Source	Relationship δ^2H =	Range δ^2H (‰)		Range $\delta^{18}O$ (‰)		*n*
		min	max	min	max	
Swale free water – wells	$2.8*\delta^{18}O - 6$	-21	-7	-5.2	0.0	25
Ridge free water – wells	$4.3*\delta^{18}O - 2$	-31	-9	-6.2	-2.5	14
Swale Soil Water	$3.0*\delta^{18}O - 5$	-37	-6	-10.1	-0.9	393
Ridge Soil Water	$3.6*\delta^{18}O - 4$	-44	0	-11.9	-1.1	390
Pond Water	$4.5*\delta^{18}O - 0$	-33	-4	-6.3	+0.2	16
Throughfall	$5.7*\delta^{18}O + 6$	-40	+11	-7.6	+4.7	162
Ridge free water – soils	$0.0*\delta^{18}O - 10$	-17	+5	-4.5	+5.8	20
Swale free water – soils	$2.1*\delta^{18}O - 8$	-21	-9	-4.5	+1.3	44

Ridge soil water isotopic composition was more heterogeneous with depth than was swale soil water (Figure 6 c-h). The average difference between shallow and deep mean isotopic composition in ridge soils was 0.4‰ for $\delta^{18}O$ for and 3‰ for δ^2H. The average difference between shallow and deep mean isotopic composition in swale soils was 0.2‰ for $\delta^{18}O$ and 0.4‰ for δ^2H. Heterogeneity was apparently related to individual events. For example, isotopically depleted throughfall from a tropical cyclone in the late summer (July 27) strongly influenced shallow soil water isotopic composition in ridge soils. The difference between shallow and deep soil water isotopic composition on the ridge persisted from August until wet-up in late-November. Swale soil water isotopic composition was also strongly affected by this event, but did not vary with depth more than usual during this period. Instead, the greatest variability in swale soil water isotopic composition with depth occurred after wet-up.

Ridge soil water was more variable than swale soil water isotopic composition laterally (within samplings of the same depth) and spatially (among soil profiles) (Figures 6 and 10). Although isotopic variation within the swale was generally low compared to the ridge, there were individual instances of high variation at all depths. Anomalously high lateral variances were not apparently related to soil water content or organic matter (Figure 11) at either site. Ridge soil water lateral variance was greater among deeper samplings, whereas swale soil water lateral variance was greater among shallower samplings. Lc-excess was more variable within samplings in ridge soils (Figure 10 e and f). Isotopic variation of soil water among samplings increased at both sites, coinciding with wet-up (Figure 12). Lateral isotopic variance also increased during the growing season at both sites, but variability was greatest in ridge soils (Figure 12).

Isotopic composition of soil water was more variable through time than free water sources (Figure 9). Of all free waters sampled, throughfall was most variable (Figure 9 and Table

1). Free water collected from within the ridge soil showed strong evidence of evaporation as indicated by low lc-excess, and was the most isotopically enriched of any non-throughfall mobile water source including ponded surface water (Figures 9 and 13). Free water collected from swale soil was less enriched in $\delta^{18}O$ and $\delta^{2}H$ than was free water collected from the ridge soil. There was also some indication that free water collected from swale soil was more consistent through time (standard deviation of 1.2‰ $\delta^{18}O$ and 2‰ $\delta^{2}H$, *n*=44) than the free water collected from ridge soils (standard deviation of 1.7‰ $\delta^{18}O$ and 6‰ $\delta^{2}H$, *n*=20). Free water collected from soils more closely resembled soil bound water at the swale site (mean difference of 0.6‰ $\delta^{18}O$ and 2‰ $\delta^{2}H$) than it did at the ridge site (mean difference of 1.3‰ $\delta^{18}O$ and 3‰ $\delta^{2}H$).

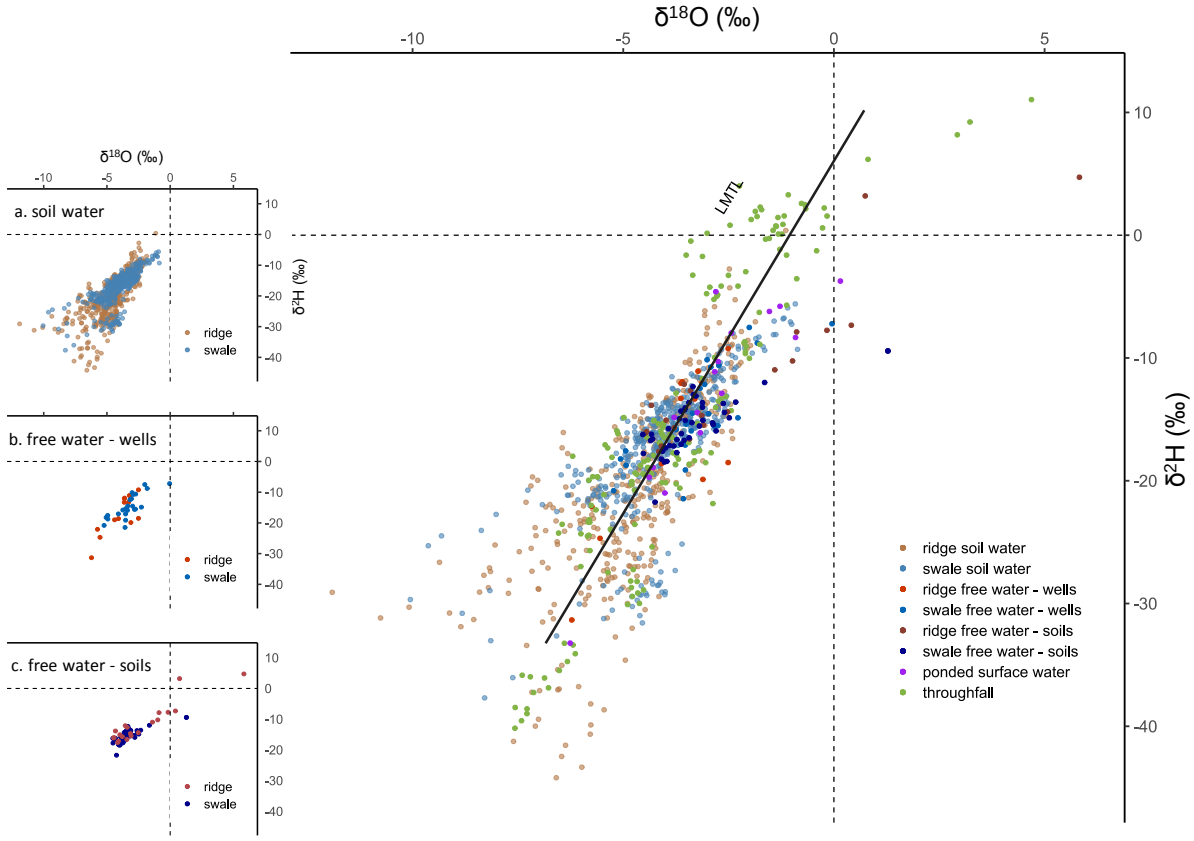

Figure 9. All water plotted in dual isotope space relative to the Local Meteoric Throughfall Line. Insets show (a) soil water, (b) free water from shallow monitoring wells, and (c) free water collected during soil excavation.

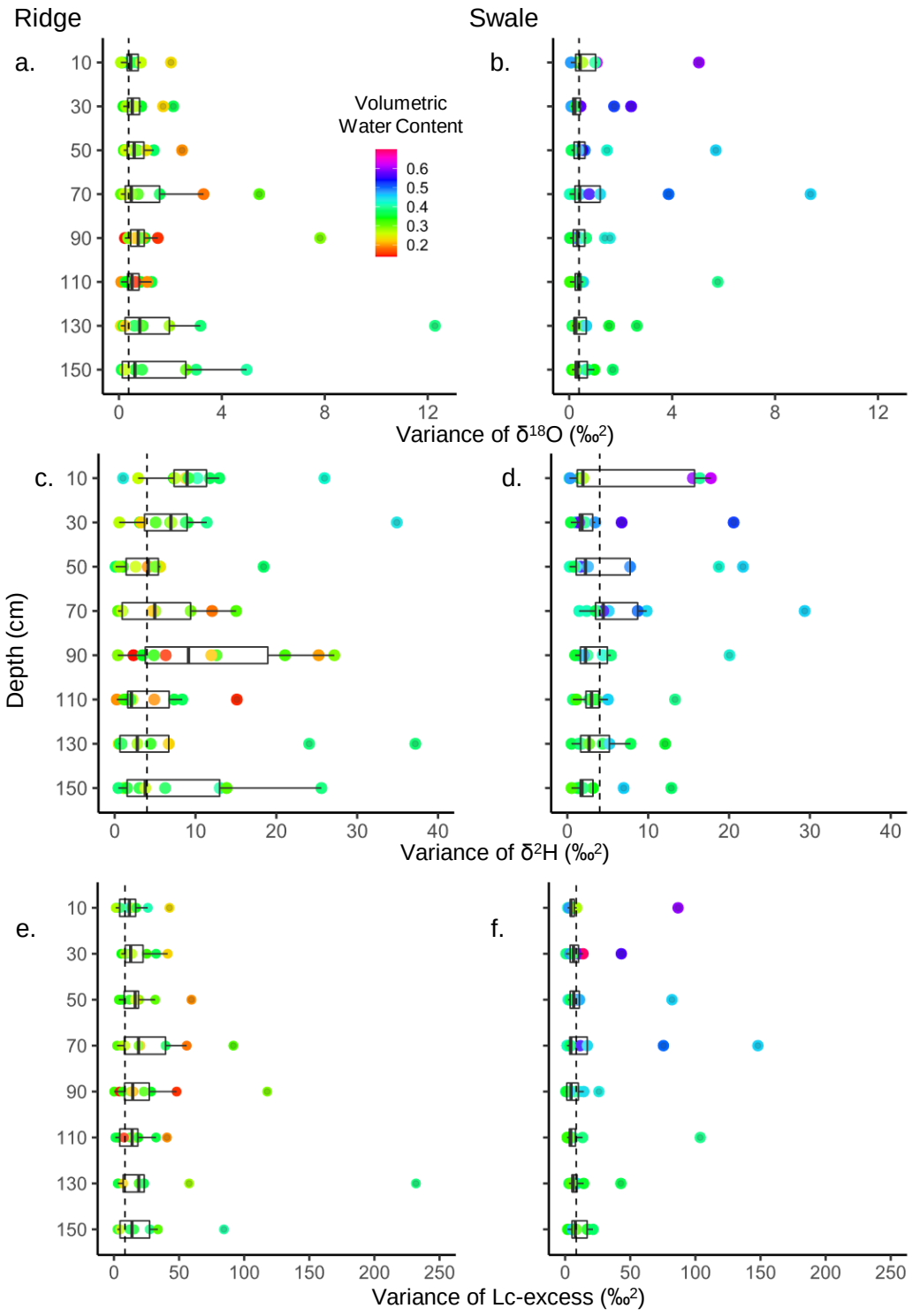

Figure 10. (a, b) Variance of $\delta^{18}O$ among soil water samples of the same depth. (c, d) Variance of $\delta^{2}H$ among soil water samples of the same depth. (e, f) Variance of lc-excess among soil water samples of the same depth. The box represents the interquartile range and the vertical bar within the box represents the median. The points are the data informing the boxplot colored by volumetric water content. The vertical dashed line represents experimental precision for each variable.

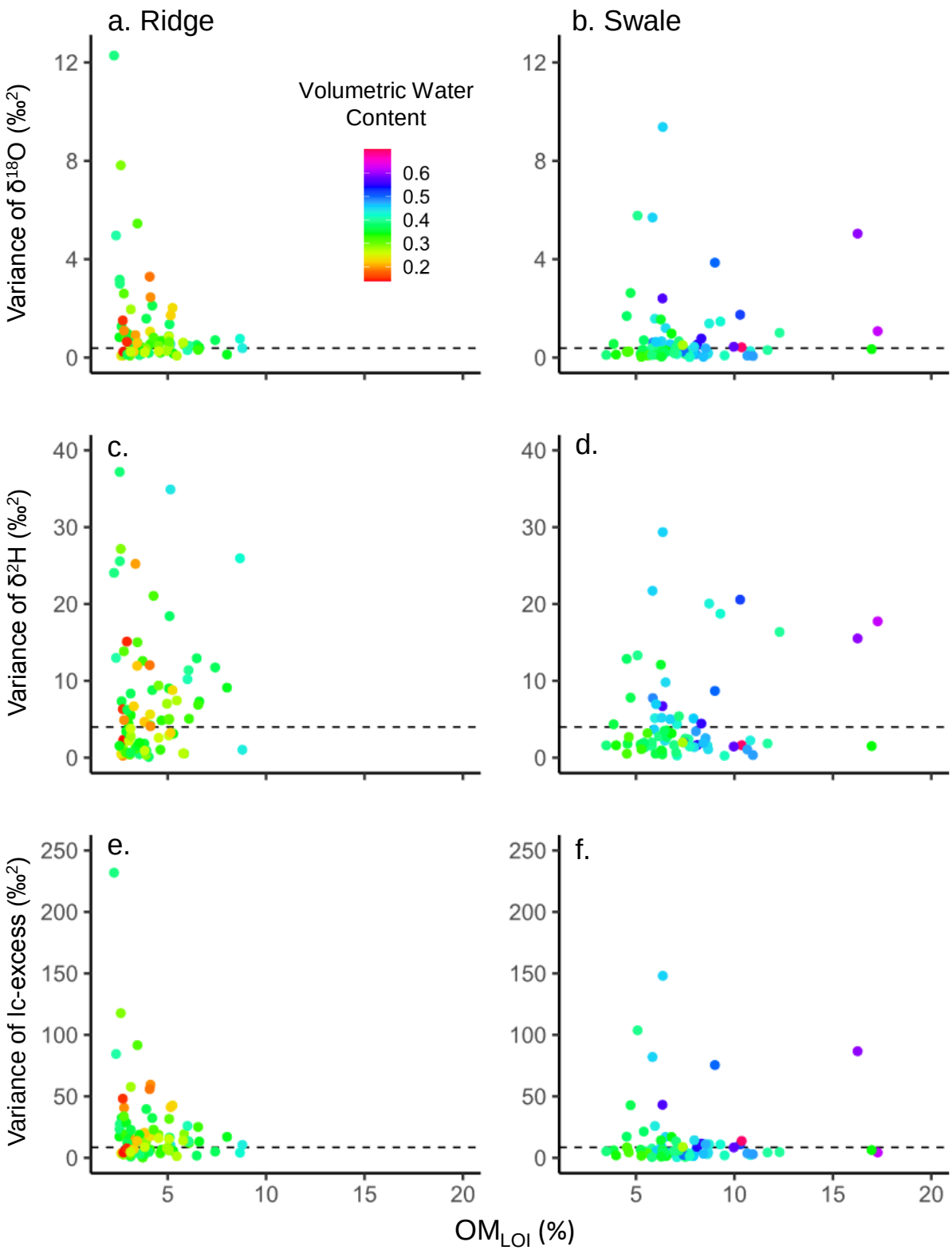

Figure 11. Variance of (a, b) $\delta^{18}O$, (c, d) $\delta^{2}H$, and (e, f) lc-excess within soil water samples by organic matter content. The points are colored by volumetric water content. The horizontal dashed lines represent experimental precision for each variable.

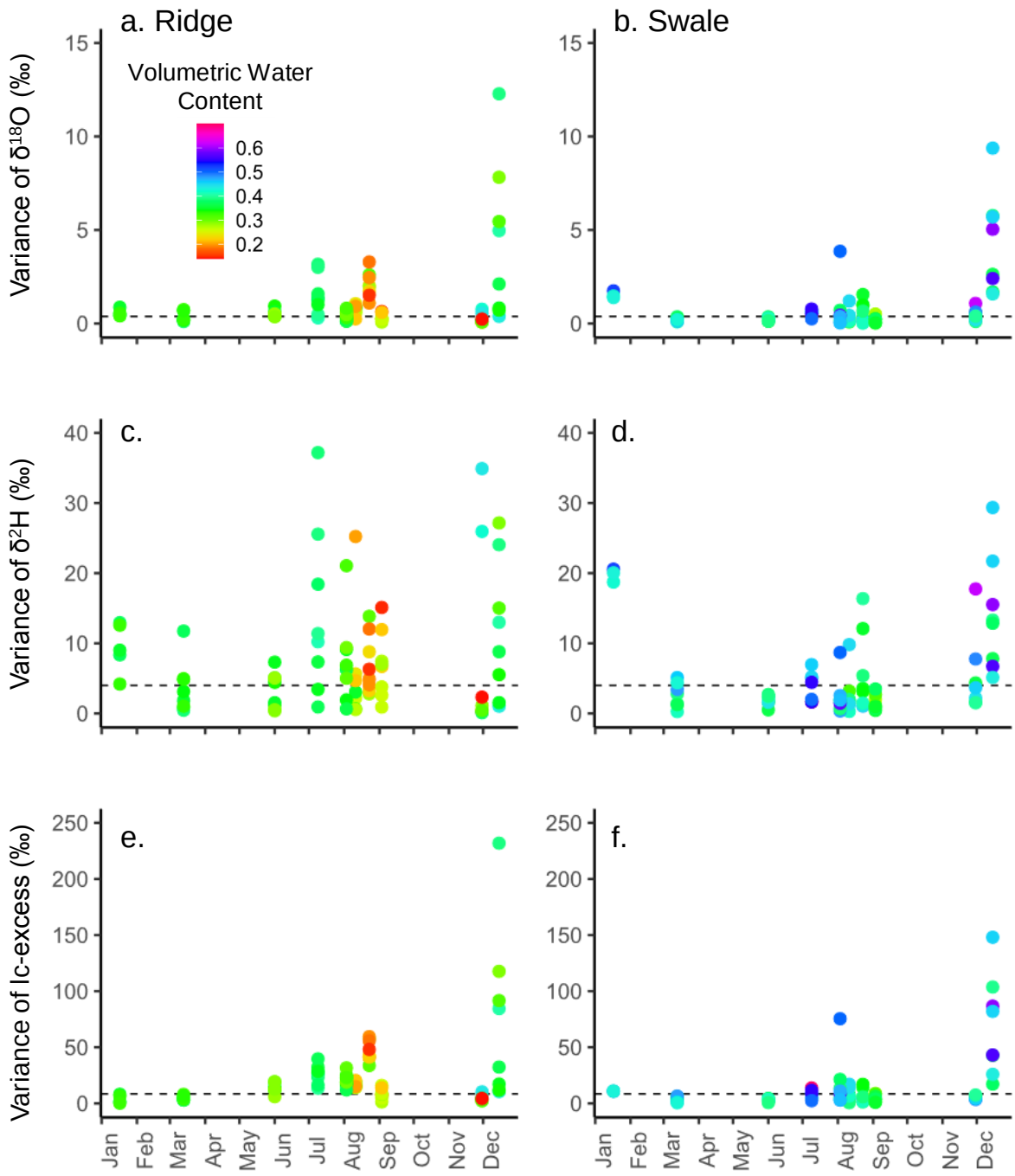

Figure 12. Time series of variance of (a, b) $\delta^{18}O$, (c, d) $\delta^{2}H$, and (e, f) lc-excess with color denoting volumetric water content. The horizontal dashed line represents experimental precision for each variable.

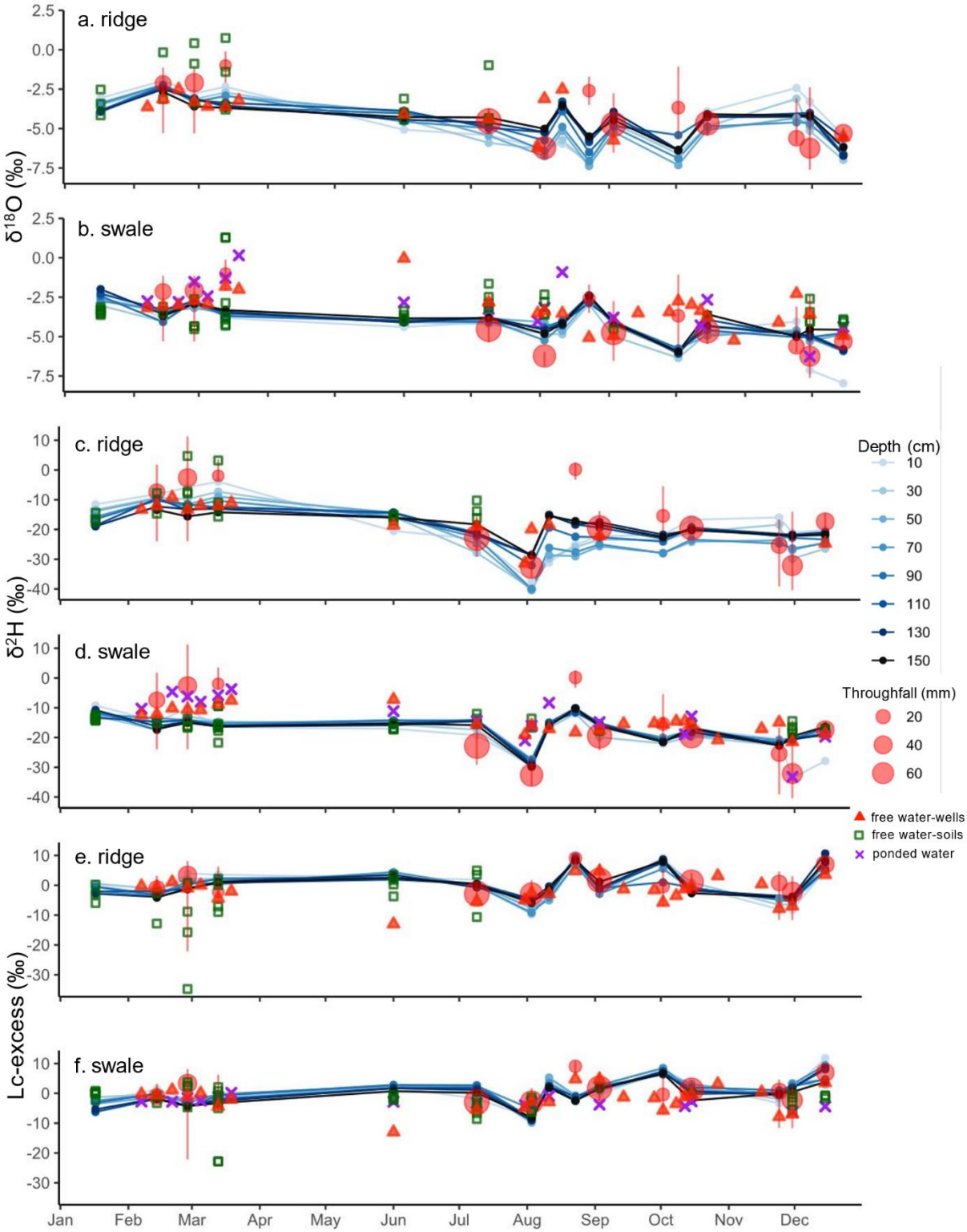

Figure 13. Isotopic composition of soil water and free water through time in the (a, c. e) ridge and (b, d, f) swale, including (a, b) $\delta^{18}O$, (c, d) $\delta^{2}H$, and (e, f) lc-excess. Blue points represent mean isotopic composition of soil water by depth. Red circles represent the weighted mean isotopic composition of throughfall and its associated amount. Vertical red lines represent the range of throughfall isotopic composition in the period prior to each sample.

Isotopic composition of ponded surface water in the swale was similar to throughfall in the winter and early spring (Figure 13). Later in the summer, it deviated from throughfall, with negative lc-excess suggesting evaporation was the cause of deviation. Similarly, notable isotopic deviations between ridge and swale free water from wells are likely attributable to differences in evaporation as indicated by lc-excess. Mean $\delta^{18}O$ and $\delta^{2}H$ did not substantially differ between ponded surface water and free water from wells.

Isotope-balance model results suggest that Replacement (soil water is the same as event water) is the best fit model for swale soil water $\delta^{18}O$ and $\delta^{2}H$, and Conservative Mixing is the best fit model for ridge soil water $\delta^{18}O$ and $\delta^{2}H$ (Figure 14). Each of the three models predict $\delta^{2}H$ at the ridge site similarly, but the Conservative Mix model had the greatest R^2. Model fit of ridge soil $\delta^{2}H$ was likely heavily influenced by a few isotopically enriched outliers. The No Exchange model (no effect of throughfall on isotopic composition) was the worst fit for the swale in both $\delta^{18}O$ and $\delta^{2}H$. The Replacement model was the worst fit for ridge. Lc-excess of swale soil was not well predicted by any of the models ($R^2 \leq 0.04$). The Replacement model was the best fit for lc-excess of ridge soil ($R^2 = 0.44$) however its slope is also heavily influenced by two values.

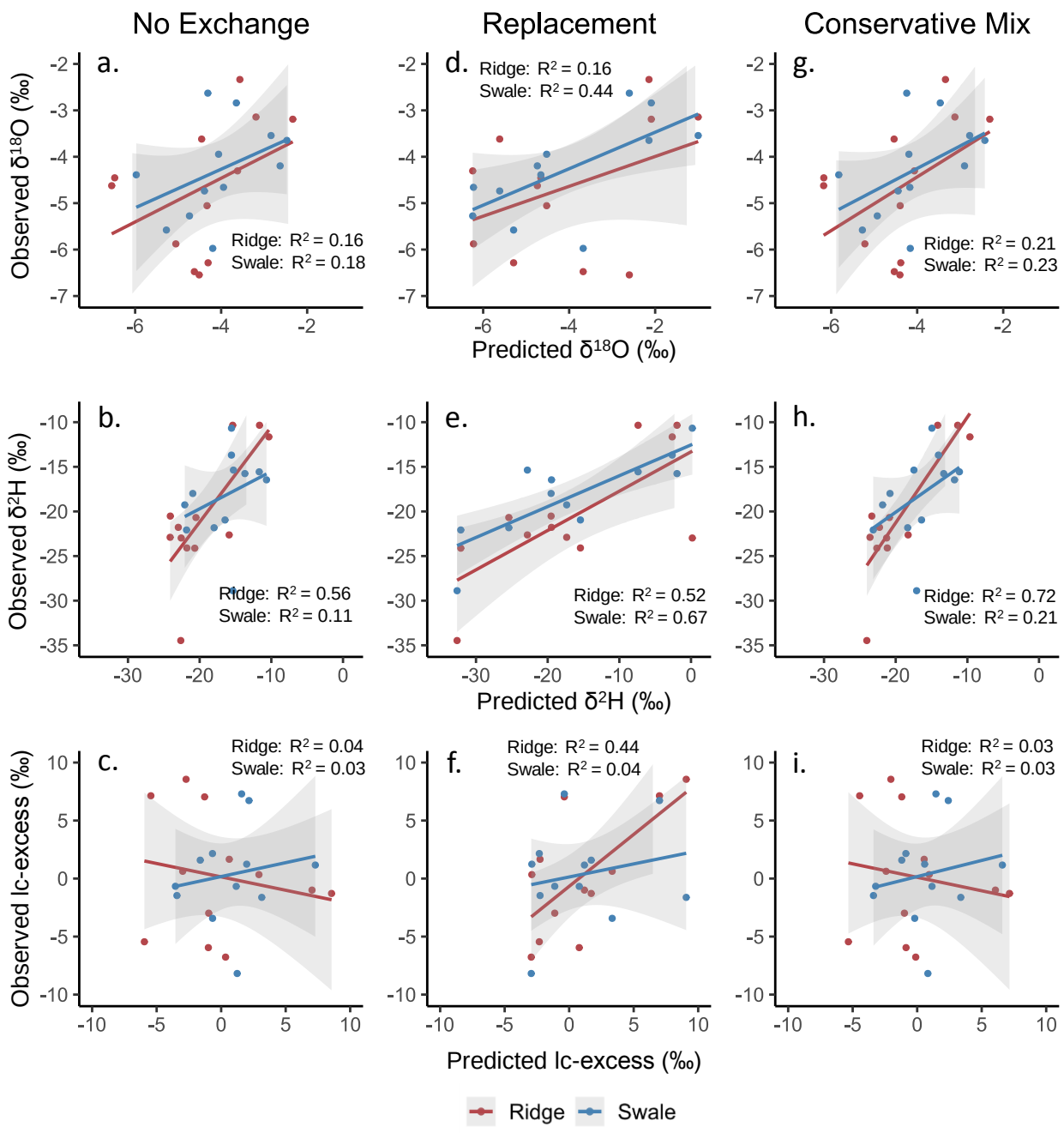

Figure 14. $\delta^{18}O$, $\delta^{2}H$, and lc-excess predictions for the ridge and swale sites based on mean soil water isotopic composition by sample date and weighted mean isotopic composition of throughfall informing each sample date. (a, b, c) Linear model of no exchange between bound water and throughfall. (d, e, f) Linear model of complete bound water replacement by throughfall. (g, h, i) Linear model of conservative mixing.

DISCUSSION

Soil water isotopic composition was more variable than throughfall isotopic composition suggesting interactions within the soil profile contributed greatly to the isotopic variability of soil water. However, the dominant factor (e.g. texture, organic matter, structure, water content) contributing to the isotopic variability of soil water was not obvious. There was no correlation between instances of high isotopic variance of soil water and greater spatial isotopic variability of throughfall, suggesting that soil water isotopic variability did not stem from variability of throughfall alone. There was no clear trend between lateral isotopic variance and soil water content (Figure 10 and 12), suggesting that preferential and heterogeneous infiltration is not be the main driver of isotopic variance within soil water. The greatest instances of soil water isotopic variance occurred when soil organic matter content was relatively low (Figure 11). This suggests that increased presence of organic matter was not a main driver of soil water isotopic variance. We used ridge soils to understand the effect of soil texture on soil water isotopic variance because ridge soil was coarser at depth. There was an increase in variance of δ^2H at the 90 cm depth interval coinciding with the textural change. However, variance did not increase in $\delta^{18}O$ and did not remain consistently high within the coarser textured range of ridge soils (90-150 cm) suggesting that variance was not predominantly associated with the change in soil texture.

Using lc-excess to characterize effects of evaporation revealed differences in the relationships between free and bound waters at each site. Free water collected from ridge soil was generally more evaporated than soil water and throughfall as indicated by lower lc-excess. Whereas, free water collected from swale soils was generally more similar to lc-excess of soil water and throughfall. There may be a greater effect of evaporation in the ridge site because the soil surface on the ridge was always drier than in the swale. When the surface of the soil is relatively dry, water deeper in the soil profile will move towards the soil surface as water vapor (Brutsaert, 2014). Repetitive vertical transport driven by evaporation through vapor pathways within the ridge site may explain lower lc-excess of mobile water through Rayleigh fractionation in which heavier isotopes (^2H and ^{18}O) persist in the reservoir (i.e. free water in soil).

Instances of positive soil water lc-excess (i.e. soil water isotope composition that plots above the LMTL) were common in this study (Figure 9), but Oct 2 was the only sampling event where soil water lc-excess was substantially greater than throughfall lc-excess. The lc-excess of free water on Oct 2 was negative at both sites while the lc-excess of soil water was positive. The maximum lc-excess of throughfall prior to this sampling event was +6.5‰, which is less than maximum lc-excess of ridge soil water (+9.1‰) or swale soil water (+8.5‰) (Figure 13). Soil water lc-excess greater than throughfall lc-excess suggests a more complex relationship between infiltration and soil water recharge since throughfall is the primary infiltrating water source.

Data in which lc-excess of soil water is greater than throughfall and other mobile waters are an interesting anomaly that may be explained by several processes, each of which has implications for understanding the dominant hydrological process. One possible reason for positive lc-excess of soil water may have been selective recharge by precipitation by less than the entirety of an event (O'Driscoll *et al*., 2005; Lemon, 2020). Isotopic composition varies during rain events, so if some precipitation after initial soil recharge bypasses soil pores, it

therefore would have less influence on soil water isotopic composition. For this hypothesis to be true, mobile waters should reflect the mean isotopic composition of precipitation which would suggest that subsequent rainfall did not mix with bound water and is instead moving as mobile flow through soil. This hypothesis holds for samplings on Oct 2 at both sites, but is not true for any other instances of positive soil water lc-excess. Furthermore, throughfall with the greatest lc-excess was collected 18 days prior to soil sampling which was the first throughfall collection informing the soil sampling on Oct 2. This throughfall fell on relatively dry soil (Figure 5) which is understood to increase the likelihood of selective recharge. The differences in lc-excess between throughfall and soil water may therefore be evidence of bypass flow occurring after initial soil water recharge (Brooks *et al*., 2010).

Selective recharge by certain portions of a throughfall event is also a likely source of soil water isotopic deviation from prediction in the simple, event-scale soil water isotope models. Replacement of soil water by throughfall was the best model fit describing lc-excess (Figure 14 f), but the observed soil water lc-excess was sometimes greater (more condensed or less evaporated) than predicted using throughfall event averages alone. Therefore, it is possible that selective recharge is ubiquitous and likely influenced other soil sampling events. But without an isotopically distinct recharging portion of the storm, the effect is not noticeable isotopically.

Another possible reason for positive lc-excess of soil water is fractionation processes within the soil that result in isotopic signatures characteristic of distillation through vapor condensation onto soil surfaces. Episaturation of soil paired with unsaturated macropores may create an ideal situation for vapor to transit through a diffusive pathway deeper into the soil profile where it then can condense onto the soil surface if temperatures there are lower (Lemon, 2020). This hypothesis is based on studies of soil temperature gradients and matric potential (Philip and De Vries, 1957; Box and Taylor, 1962) and builds upon our understanding of how macropores facilitate diffusion, especially in structured soils. For positive soil water lc-excess to be a result of vapor condensation, we would expect to see a relationship of lc-excess and depth. It would be more likely for soils at depth to be isotopically depleted and with positive lc-excess as warm, moist vapor transits into deeper soil through unsaturated macropores and condenses onto cooler soil particles. However, there was no relationship between lc-excess and soil depth during samplings on Oct 2 (when lc-excess of soil water was greater than lc-excess of throughfall) and temperature gradients may also not have been conductive (no data available).

Lc-excess of soil water was often more heterogenous within a single sampling event than the throughfall informing it. We expected effects of kinetic fractionation on isotopic composition of soil water to be identifiable using lc-excess because we expected differences in lc-excess between events to be driven by throughfall lc-excess and evaporation between events. However, physical and temporal variability in lc-excess made patterns hard to interpret. There was variability of soil water lc-excess within sampling events, between sites, with depth (Figure 6 g and h), and among samples of the same depth class (Figure 10). Soil water lc-excess at both sites became increasingly more variable with depth during initial wet-up in December, suggesting lc-excess might be related to soil structure. If, as expected, macropores increase evaporation rates in low-permeability soils with connectivity to shallow groundwater by increasing soil moisture

(Zhou *et al*., 2020), soil structural changes (such as shrinking and swelling of vertisols) would then likely also affect soil water lc-excess.

Soil water isotope data from seasonal wet-up suggests that soil structure is the dominant factor influencing soil water isotopic variability among samples of the same depth. Data from samplings in December are the best proxy for change in soil structure from dry to wet, with attendant closure of cracks in the vertic soil. During this timeframe, swale soils became episaturated and the macropore network within the swale was likely altered. Wet-ups following a period of low antecedent soil water content are more likely to create a poorly hydrologically connected, variably perched macropore network (Lemon, 2020) in which flow is preferential through discontinuous voids (Bouma *et al*., 1980). Given the way infiltration occurs in vertic soils, it is possible that mobile water (throughfall and surface run-on) entered and percolated through variably connected, surface macropores during initial wet-up (Bouma and Dekker, 1978; Beven and Germann, 1982). Following wet-up, the swale soil likely swelled effectively limiting further percolation, resulting in greater variability of free water isotopic composition within soils. The discontinuity of the macropore network after wet-up and subsequent diffusion into the soil matrix may explain greater lateral soil water isotopic variance in December.

Several pieces of evidence suggest that lateral hydrologic exchange occurs between the ridge and swale sites. Water level data suggest surface water in the swale likely subsidized ridge soils during periods of high groundwater elevation in the swale. The opposite seems to be true during times of low groundwater elevation in the swale. The evidence implying lateral hydrologic exchange between sites includes the gradient in groundwater levels (Figure 4) and soil water isotopic composition during some sampling periods, when water in ridge soils at depth more closely resembled soil water isotopic composition in the swale (Figure 6). The topography of the study area makes it so that the surface of the swale is approximately laterally adjacent to ridge soils at 130 cm depth. Therefore, ridge soils at depth would be expected to have greater hydrological connection to the surface of the swale than ridge soil near the surface. Some individual responses of soil water isotopes to events further suggest lateral connectivity between sites. For example, ridge soil samples collected on Aug 3, following a tropical cyclone were more depleted in ^{2}H near the surface than at depth. By the next soil sampling on Aug 11, ridge soil water at depth was more comparable to the $\delta^{2}H$ of swale soil than shallow ridge soil water, even though the study area did not receive any throughfall between the two sampling periods (Figure 6).

The role of groundwater below sampling depth is not well constrained but seems to be apparent in soil moisture and soil water isotopic variability. Swale groundwater isotopic composition was always similar to throughfall isotopic composition (figure 13), suggesting that precipitation recharges groundwater at the swale site likely through deep drainage. Swale soil water isotopic composition was responsive to individual throughfall events, yet there were no distinct isotopic differences with depth in swale soils, suggesting greater hydrological connectivity of groundwater at the swale site than at the ridge site. Greater connectivity of groundwater to swale soils than ridge soils may be due to a greater presence of macropores at the swale site (which were often visible at the surface) (Beven and Germann, 1982; Zhou *et al*.,

2020) and greater capacity for capillary rise in cohesive clay soils (Richards, 1931). Isotopic composition of soil water in the swale was therefore more stable through time as it was likely connected to a larger reservoir. For example, swale soil water isotopic composition returned to pre-tropical cyclone soil water isotopic composition on Aug 11 faster than ridge soils (Figure 6), suggesting a larger and more isotopically well-mixed water source recharging swale soils.

Temporal variability of ridge soil water isotopic composition was greater at the surface than at depth (Figure 6). Mean (across samples) ridge soil water isotopic composition at depth was more stable through time (Figure 13), however isotopic variance among those samples was greater than near the surface (Figure 10). This may be additional evidence of recharge only reaching certain portions of the soil at depth, as is expected when macroporosity dominates soil water flux (Weiler and Fluhler, 2004). Alternatively, the higher variance at depth may indicate variable connections to groundwater and lateral subsidies from the swale.

Soil water isotopic composition of structured soils was expected to be highly isotopically variable due to mobile flow through macropores. However, results of this study at the swale site suggest the opposite. Although swale soils are highly structured, with macropore conductivity much higher than the matrix (Gerke, 2006), swale soil water isotopic composition remained relatively homogenous with depth and space as compared to ridge soils and source waters. One likely reason for this divergence from expectation is the hydrologic regime of the swale site. Run-on from upslope into the swale, as well as possibly greater connectivity with groundwater, may have overwhelmed the expected high variability caused by structured flow. Simply being exposed to more event water could be the reason swale soil water isotopic composition appears to be more stable through time.

The simple linear mixing model of soil water content (Figure 7) provided limited information on site hydrology alone, but when paired with groundwater level (Figure 4) and soil moisture (Figure 5), predictions of soil water content became more informative. Information from the site water budgets suggest that lateral hydrologic subsidies may bridge gaps in predictions of soil water content. There were several sampling dates in which swale soil water content was underpredicted. Water content of swale soil was likely more difficult to predict (lower R^2), likely because the linear mixing model did not include any terms for subsurface lateral exchange, free water at the surface of the swale, runon from upslope, or deep drainage, so the assumptions (section 3.4) were likely oversimplified. We expected our predictions of water content in the swale to be most affected by subsurface lateral exchange and surface runon due to the topography of the study area and the general nature of infiltration in forest soils. Taking this information into account, volumetric water content during certain samplings may better be explained with reference to other data. For example, swale soil water content was underestimated by 38 mm and ridge soil water content was overestimated by 46 mm on Aug 23. It is possible that the ridge site was contributing water to the swale site in the form of surface runoff since groundwater level at both sites responded to a precipitation event (Figure 4) that occurred 10 days prior to soil sampling and it is unlikely that all event water infiltrated into ridge soils. When ridge soils were dry, the water balance model indicates that the swale subsidized the ridge, similar to other evidence of lateral soil water isotopic exchange between sites discussed earlier.

For example, the water balance model underestimated water content in ridge soils by 44 mm and overestimated swale soils by 41 mm on Nov 24. For this sampling event, lateral exchange could close the gaps between predicted and observed soil water content.

Data quality issues within the water budget may have influenced interpretation of the model of soil water content. For example, lateral subsidies may close the gaps in the water budget on Nov 24, but less soil water content information was available overall on this collection date due to sampling issues. Dry soil conditions at the ridge site made it difficult to extract samples from depth, so there are only 4 soil samples informing the observed mean water content of ridge soils on this date. Other data quality issues within the model of soil water content stem from calculation of throughfall amount at the study area. We used the sum of precipitation between soil sampling events from a nearby rain gauge and a constant 20% rate of interception loss because our throughfall samplers at the study area occasionally undercaught throughfall. This throughfall calculation method makes it so that the resulting model is not sensitive to potential variation in interception rates which impacts the accuracy of our predictions.

This study evaluated models of soil water isotopic composition that represented ideal scenarios to constrain soil hydrological process at each site. The No Exchange and Replacement models represent opposite alternative hypotheses for the hypothesis of conservative mixing. The No Exchange model is the closest to the framework of the Two Water Worlds hypothesis, represented by complete bypass flow in which the soil matrix does not exchange with incoming mobile event water. The Replacement model represents complete replacement of bound soil water with incoming mobile event water – a violation of conservation of mass in most study periods but still a useful null for comparison. The Conservative Mix model represents a middle ground in which the prior soil water and incoming event water mix proportionally.

Conflicting soil water isotope model results between the two sites (i.e., Replacement in the swale vs Conservative Mixing in the ridge) may suggest different soil water recharge regimes: event-driven replacement in swale soils and conservative mixing in ridge soils. Greater lateral and spatial isotopic variance within ridge soils likely accounts for disparities between predicted and observed soil water isotopic composition. Ridge soil bound water isotopic composition cannot be easily predicted in these models due to greater observed spatial, vertical, and temporal variability (Figures 6, 10, and 12) that cannot be reproduced by mean values alone.

Throughfall undercatch and limited sensitivity of throughfall quantity in modeling has implications on isotope model results. Lapses in throughfall collection between soil sampling events sometimes resulted in undercatch, but with full samplers. For this reason, it is likely that throughfall isotopic composition is likely biased towards the beginning of the collection period informing the soil sampling, and subsequent throughfall isotopic composition is unknown and not equally represented in mean throughfall isotopic composition. Additionally, soil water isotopic modeling was not highly sensitive to estimates of quantity (e.g. the estimated throughfall quantities) because the amount of soil water was always greater than the amount of throughfall. All three model scenarios for lc-excess were poor representations of soil water isotopic process. One possibility is that predictions of lc-excess are insufficient because each lc-excess model

inherits errors in the prediction of $\delta^{18}O$ and $\delta^{2}H$ which is subsequently compounded in models of lc-excess. (Figure 13).

The soil water content data and isotopic data implied apparently conflicting conclusions about hydrological processes in the swale. During periods of saturation vertic soils swell, which limits connectivity with groundwater at depth and promotes episaturation (Lin *et al*., 1998; Or *et al*., 2000; Das Gupta *et al*., 2006). Although this phenomenon was evident in the swale soil water content decreasing with depth, it was not evident isotopically. The only sampling periods in which isotopic compositions of swale soils strongly varied with depth were during wet-up in December. Results from this study thus appear to conflict with previous findings of high isotopic variability in structured clay soils. Morales *et al,* (2021) demonstrated that vertic soils did not fully resolve to equilibrium with flood water isotopic composition even after a prolonged period of inundation (31 days) as a result of nonconductive macropores and slow molecular diffusion. However, results from our study indicate samplings during periods in which ponded surface water was visible (and soil was likely swollen) were generally similar to samplings without ponded water influence. The most likely explanation for this apparent conflict is that the scale of measurement was different in this study (20 cm^3) than the small (3 cm^3) peds analyzed by Morales *et al.,* 2021, so that heterogeneities at smaller scales became integrated and masked.

Problems arise when attempting to up or down-scale information from this study, since heterogeneities become apparent at different observational scales (Bloschl and Sivapalan, 1995). There was discernable isotopic variance in ridge soils within the 1 m^2 spatial scale and 20 cm depth resolution, but isotopic variance was not as apparent in swale soils except during initial wet-up in the winter where high soil water isotopic variability was observed with depth. Results of this study made progress toward constraining the factors affecting soil water isotopic variability, but we still cannot clearly identify all major factors contributing to variance from the resolution of data collected**.** Research constraining isotopic variability in natural systems should focus efforts into observing processes at the same scale that they occur (Bloschl and Sivapalan, 1995) ideally in a way that can generalize findings while simultaneously highlighting heterogeneities (Harte, 2002) – but in soil water fluxes the relevant scale remains poorly understood. McDonnell *et al*., (2007) suggested focusing on heterogeneities that emerge at various scales and their related hydrological effects. Although this study provides context as to what heterogeneities are integrated across at the local scale, it is possible that heterogeneities in swale soils were not as evident as in ridge soils as a result of scale issues in sampling. For example, it is possible that heterogeneities in swale soils may increase and heterogeneities in ridge soils may decrease on a larger spatial scale.

CONCLUSIONS

Spatiotemporal sampling of a ridge-swale topographic forest revealed two major soil water recharge regimes at the profile scale: event-driven (i.e. throughfall and event run-on) replacement in swale soils and conservative mixing in ridge soils. However, individual soil water isotopic composition greatly deviated from model predictions. The bound water isotopic composition was relatively much less variable through time and space within structured swale soils as compared to ridge soils. Soil hydrological connectivity with larger water sources (e.g. surface water and groundwater) is likely responsible for bound water isotopic stability through time in the swale and in ridge soils at depth as a result of lateral subsidies between sites. There was no strong relationship between soil water isotopic variability and soil water content, organic matter, or texture. Instead, the timing of soil water isotopic variance seems to be related to soil structure and hydrologic processes that varied by geomorphic position.

APPENDIX A. SUPPLEMENTARY FIGURES

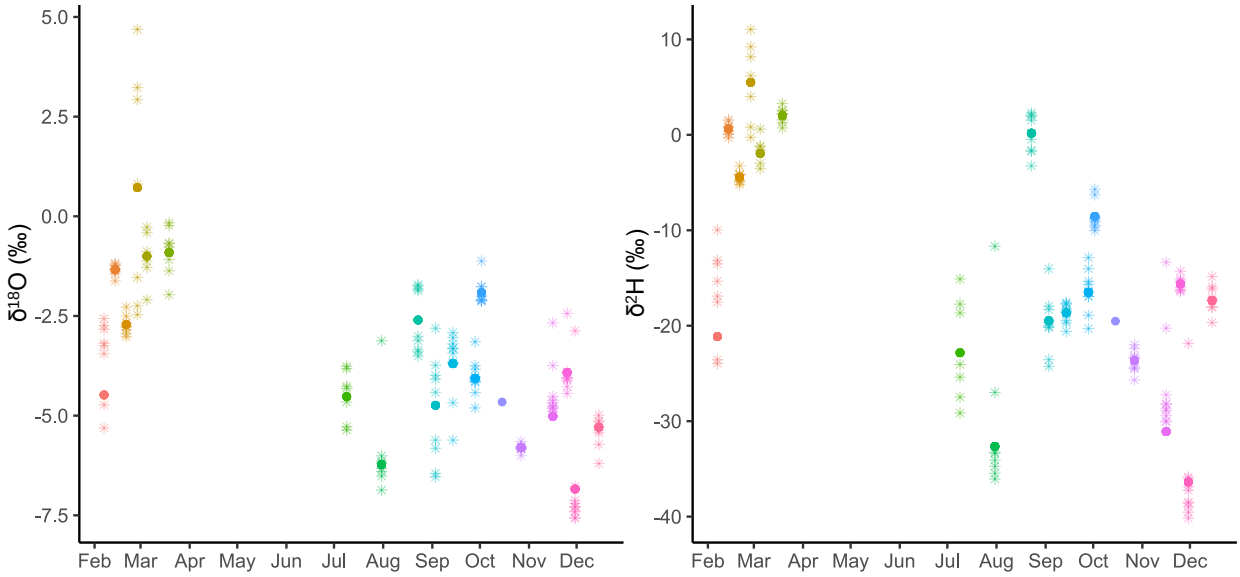

Figure A1. Time series of throughfall isotopic composition. Asterisks represent composition of individual throughfall collectors and circles represent the volume-weighted average.

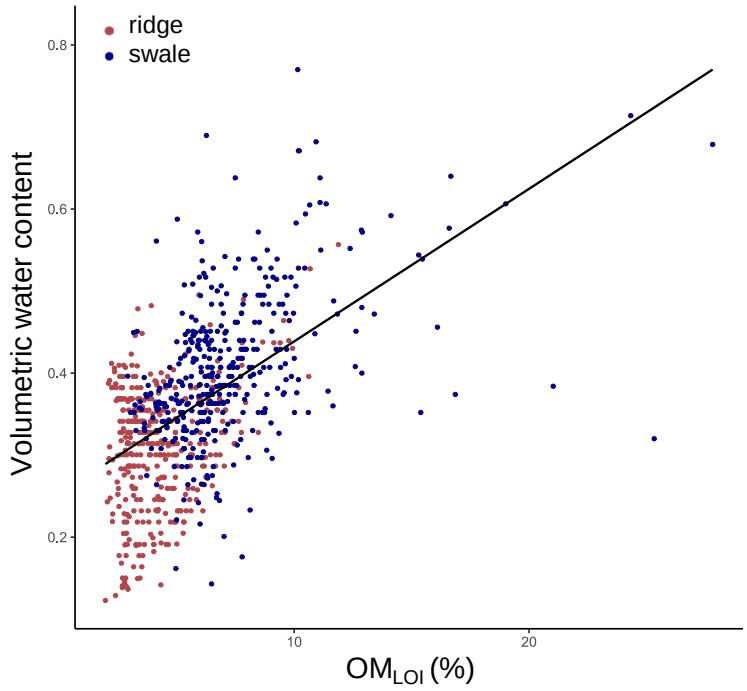

Figure A2. Relationship of soil volumetric water content and OM_{LOI} ($R^2 = 0.31$).

Figure A3. Swale sampling site with ponded surface water.

Figure A4. Image of free water flowing from a root channel at the swale site that was intercepted when digging a borehole for soil collection.

Figure A5. Soil surface cracking in the swale in late August, 2020.

Figure A6. Mottled soil sample from swale site.

REFERENCES

Aggarwal, P. K., Araguas-Araguas, L., Groning, M., Kulkarni, K.M., Kurttas, T., Newman, B.D., Tanweer, A. (2009). *Laser Spectroscopic Analysis of Liquid Water Samples for Stable Hydrogen and Oxygen Isotopes*. Vienna: International Atomic Energy Agency.

Allen, S. T., Keim, R. F., Barnard, H. R., McDonnell, J. J., & Renée Brooks, J. (2017). The role of stable isotopes in understanding rainfall interception processes: a review. *WIREs Water*, *4*(1), e1187.

Allen, S. T., Kirchner, J. W., Braun, S., Siegwolf, R. T. W., & Goldsmith, G. R. (2019). Seasonal origins of soil water used by trees. *Hydrology and Earth System Sciences*, *23*(2), 1199-1210.

Ball, D. F. (1964). Loss-on-ignition as an estimate of organic matter and organic carbon in non-calcareous soils. *Journal of Soil Science*, *15*(1), 84-92.

Barnes, C. J., & Allison, G. B. (1988). Tracing of water movement in the unsaturated zone using stable isotopes of hydrogen and oxygen. *Journal of Hydrology*, *100*(1), 143-176.

Bendix, J., & Hupp, C. R. (2000). Hydrological and geomorphological impacts on riparian plant communities. *Hydrological Processes*, *14*(16- 17), 2977-2990.

Berghuijs, W. R., & Allen, S. T. (2019). Waters flowing out of systems are younger than the waters stored in those same systems. *Hydrological Processes*, *33*(25), 3251-3254.

Berry, Z. C., Evaristo, J., Moore, G., Poca, M., Steppe, K., Verrot, L., . . . McDonnell, J. (2018). The two water worlds hypothesis: Addressing multiple working hypotheses and proposing a way forward. *Ecohydrology*, *11*(3).

Beuselinck, L., Govers, G., Poesen, J., Degraer, G., & Froyen, L. (1998). Grain-size analysis by laser diffractometry: comparison with the sieve-pipette method. *CATENA*, *32*(3), 193-208.

Blöschl, G., & Sivapalan, M. (1995). Scale issues in hydrological modelling: A review. *Hydrological Processes*, *9*(3-4), 251-290.

Bouma, J., & Dekker, L. W. (1978). A case study on infiltration into dry clay soil. Morphological observations. *Geoderma*, *20*(1), 27-40.

Bouma, J. (1981). Soil morphology and preferential flow along macropores. *Agricultural Water Management*, *3*(4), 235-250.

Bowen, G. J., Kennedy, C. D., Liu, Z., & Stalker, J. (2011). Water balance model for mean annual hydrogen and oxygen isotope distributions in surface waters of the contiguous United States. *Journal of Geophysical Research: Biogeosciences*, *116*(G4).

Bowen, G. J., & Good, S. P. (2015). Incorporating water isoscapes in hydrological and water resource investigations. *WIREs Water*, *2*(2), 107-119.

Bowers, W. H., Mercer, J. J., Pleasants, M. S., & Williams, D. G. (2020). A combination of soil water extraction methods quantifies the isotopic mixing of waters held at separate tensions in soil. *Hydrology and Earth System Sciences*, *24*(8), 4045-4060.

Bowling, D. R., Schulze, E. S., & Hall, S. J. (2017). Revisiting streamside trees that do not use stream water: can the two water worlds hypothesis and snowpack isotopic effects explain a missing water source? *Ecohydrology*, *10*(1), e1771.

Box, J. E., & Taylor, S. A. (1962). Influence of soil bulk density on matric potential. *Soil Science Society of America Journal*, *26*(2), 119-122.

Brantley, S. L., Goldhaber, M. B., & Ragnarsdottir, K. V. (2007). Crossing disciplines and scales to understand the critical zone. *Elements*, *3*(5), 307-314.

Brooks, J. R., Barnard, H. R., Coulombe, R., & McDonnell, J. J. (2010). Ecohydrologic separation of water between trees and streams in a Mediterranean climate. *Nature Geoscience*, *3*(2), 100-104.

Brutsaert, W. (2014). Daily evaporation from drying soil: Universal parameterization with similarity. *Water Resources Research*, *50*(4), 3206-3215.

Bryant, M. L., Bhat, S., & Jacobs, J. M. (2005). Measurements and modeling of throughfall variability for five forest communities in the southeastern US. *Journal of Hydrology*, *312*(1-4), 95-108.

Cain, M. R., Ward, A. S., & Hrachowitz, M. (2019). Ecohydrologic separation alters interpreted hydrologic stores and fluxes in a headwater mountain catchment. *Hydrological Processes*, *33*(20), 2658-2675.

Cassel, D. K., & Nielsen, D. R. (1986). Field Capacity and Available Water Capacity. In A. Klute (Ed.), *Methods of Soil Analysis* (pp. 901-926).

Das Gupta, S., Mohanty, B. P., & Köhne, J. M. (2006). Soil hydraulic conductivities and their spatial and temporal variations in a vertisol. *Soil Science Society of America Journal*, *70*(6), 1872-1881.

Dawson, T. E., & Ehleringer, J. R. (1991). Streamside trees that do not use stream water. *Nature*, *350*(6316), 335-337.

Dean, W. E. (1974). Determination of carbonate and organic matter in calcareous sediments and sedimentary rocks by loss on ignition; comparison with other methods. *Journal of Sedimentary Research*, *44*(1), 242-248.

De Miranda, R. A. C., & Butler, D. R. (1986). Interception of rainfall in a hedgerow apple orchard. *Journal of Hydrology, 87*(3), 245-253.

Dubbert, M., Caldeira, M. C., Dubbert, D., & Werner, C. (2019). A pool-weighted perspective on the two-water-worlds hypothesis. *New Phytologist*, *222*(3), 1271-1283.

Evaristo, J., Jasechko, S., & McDonnell, J. J. (2015). Global separation of plant transpiration from groundwater and streamflow. *Nature*, *525*(7567), 91-94.

Gaj, M., Kaufhold, S., Koeniger, P., Beyer, M., Weiler, M., & Himmelsbach, T. (2017). Mineral mediated isotope fractionation of soil water. *Rapid Communications in Mass Spectrometry*, *31*(3), 269-280.

Gaj, M., & McDonnell, J. (2019). Possible soil tension controls on the isotopic equilibrium fractionation factor for evaporation from soil. *Hydrological Processes*.

Gazis, C., & Feng, X. (2004). A stable isotope study of soil water: Evidence for mixing and preferential flow paths. *Geoderma*, *119*, 97-111.

Gee, H. K., King, S. L., & Keim, R. F. (2014). Tree growth and recruitment in a leveed floodplain forest in the Mississippi River Alluvial Valley, USA. *Forest Ecology and Management*, *334*, 85-95.

Gerke, H. H. (2006). Preferential flow descriptions for structured soils. *Journal of Plant Nutrition and Soil Science*, *169*(3), 382-400.

Goldsmith, G. R., Muñoz- Villers, L. E., Holwerda, F., McDonnell, J. J., Asbjornsen, H., & Dawson, T. E. (2012). Stable isotopes reveal linkages among ecohydrological processes in a seasonally dry tropical montane cloud forest. *Ecohydrology*, *5*(6), 779-790.

Goldsmith, G. R., Allen, S. T., Braun, S., Engbersen, N., González- Quijano, C. R., Kirchner, J. W., & Siegwolf, R. T. (2019). Spatial variation in throughfall, soil, and plant water isotopes in a temperate forest. *Ecohydrology*, *12*(2), e2059.

Good, S. P., Noone, D., & Bowen, G. (2015). Hydrologic connectivity constrains partitioning of global terrestrial water fluxes. *Science*, *349*(6244), 175-177.

Gralher, B., Herbstritt, B., Weiler, M., Wassenaar, L. I., & Stumpp, C. (2018). Correcting for biogenic gas matrix effects on laser- based pore water- vapor stable isotope measurements. *Vadose Zone Journal*, *17*(1), 1-10.

Harte, J. (2002). Toward a Synthesis of the Newtonian and Darwinian Worldviews. *Physics Today*, *55*(10), 29-35.

Heiri, O., Lotter, A. F., & Lemcke, G. (2001). Loss on ignition as a method for estimating organic and carbonate content in sediments: reproducibility and comparability of results. *Journal of Paleolimnology*, *25*(1), 101-110.

Hendry, M. J., Schmeling, E., Wassenaar, L. I., Barbour, S. L., & Pratt, D. (2015). Determining the stable isotope composition of pore water from saturated and unsaturated zone core: improvements to the direct vapour equilibration laser spectrometry method. *Hydrology and Earth System Sciences*, *19*(11), 4427-4440.

Hewlett, J. D., & Hibbert, A. R. (1967). Factors affecting the response of small watersheds to precipitation in humid areas. In W. E. Sopper & H. W. Lull (Eds.), *Forest Hydrology* (pp. 275–290). New York: Pergamon Press.

Horton, J., & Hawkins, R. (1965). Flow path of rain from the soil surface to the water table. *Soil Science*, *100*(6), 377-383.

Hsueh, Y. H., Allen, S. T., & Keim, R. F. (2016). Fine- scale spatial variability of throughfall amount and isotopic composition under a hardwood forest canopy. *Hydrological Processes*, *30*(11), 1796-1803.

Jarvis, N. J. (2007). A review of non-equilibrium water flow and solute transport in soil macropores: principles, controlling factors and consequences for water quality. *European Journal of Soil Science*, *58*(3), 523-546.

Jasechko, S., Sharp, Z. D., Gibson, J. J., Birks, S. J., Yi, Y., & Fawcett, P. J. (2013). Terrestrial water fluxes dominated by transpiration. *Nature*, *496*(7445), 347-350.

Jena, R., Ramasamy, J., & Sivasamy, R. (2013). Analogy of Soil Parameters in Particle Size Analysis through Laser Diffraction Techniques. *Indian Journal of Hill Farming*, *26*, 78-83.

Keim, R. F., Skaugset, A. E., & Weiler, M. (2005). Temporal persistence of spatial patterns in throughfall. *Journal of Hydrology*, *314*(1-4), 263-274.

King, S. L., Sharitz, R. R., Groninger, J. W., & Battaglia, L. L. (2009). The ecology, restoration, and management of southeastern floodplain ecosystems: A synthesis. *Wetlands*, *29*(2), 624-634.

Klemeš, V. (1983). Conceptualization and scale in hydrology. *Journal of Hydrology*, *65*(1-3), 1-23.

Klute, A., (Ed.). 1986. *Methods of Soil Analysis Part 1- Physical and Mineralogical Methods. Second Edition.* American Society and Soil Science Society of America Book Series: 5, Madison, Wisconsin USA.

Kung, K.-J. S., Steenhuis, T. S., Kladivko, E. J., Gish, T. J., Bubenzer, G., & Helling, C. S. (2000). Impact of preferential flow on the transport of adsorbing and non-adsorbing tracers. *Soil Science Society of America Journal*, *64*(4), 1290-1296.

Landon, M., Delin, G., Komor, S., & Regan, C. (1999). Comparison of the stable-isotopic composition of soil water collected from suction lysimeters, wick samplers, and cores in a sandy unsaturated zone. *Journal of Hydrology*, *224*(1-2), 45-54.

Landwehr, J., & Coplen, T. (2006). *Line-conditioned excess: a new method for characterizing stable hydrogen and oxygen isotope ratios in hydrologic systems.* Paper presented at the International conference on isotopes in environmental studies.

Landwehr, J. M., and T. B. Coplen (2006), Line-conditioned excess: A new method for characterizing stable hydrogen and oxygen isotope ratios in hydrologic systems. *International Conference on Isotopes in Environmental Studies*, 132– 135, IAEA, Vienna.

Lemon, M. G. (2020). *Characterization of shallow subsurface hydrology in large fine-grained floodplains* [Doctoral dissertation, Louisiana State University]. LSU Digital Commons.

Leuning, R., Zhang, Y. Q., Rajaud, A., Cleugh, H., & Tu, K. (2008). A simple surface conductance model to estimate regional evaporation using MODIS leaf area index and the Penman-Monteith equation. *Water Resources Research*, *44*(10).

Lin, H., Mclnnes, K., Wilding, L., & Hallmark, C. (1998). Macroporosity and initial moisture effects on infiltration rates in vertisols and vertic intergrades. *Soil science*, *163*(1), 2-8.

Lin, Y., & Horita, J. (2016). An experimental study on isotope fractionation in a mesoporous silica-water system with implications for vadose-zone hydrology. *Geochimica et Cosmochimica Acta*, *184*, 257-271.

Liu, Y., Fang, Y., Hu, H., Tian, F., Dong, Z., & Khan, M. Y. A. (2020). Ecohydrological Separation Hypothesis: Review and Prospect. *Water*, *12*(8), 2077.

Majoube, M. (1971). Fractionation of oxygen 18 and deuterium between water and its vapor (In French). *Journal de Chimie Physique*, *68*, 1423-1436.

McDonnell, J. J., Sivapalan, M., Vaché, K., Dunn, S., Grant, G., Haggerty, R., . . . Weiler, M. (2007). Moving beyond heterogeneity and process complexity: A new vision for watershed hydrology. *Water Resources Research*, *43*(7).

McDonnell, J. J. (2014). The two water worlds hypothesis: ecohydrological separation of water between streams and trees? *WIREs Water*, *1*(4), 323-329.

Mertes, L. A. K. (1997). Documentation and significance of the perirheic zone on inundated floodplains. *Water Resources Research*, *33*(7), 1749-1762.

Metzger, J. C., Wutzler, T., Dalla Valle, N., Filipzik, J., Grauer, C., Lehmann, R., . . . Hildebrandt, A. (2017). Vegetation impacts soil water content patterns by shaping canopy water fluxes and soil properties. *Hydrological Processes*, *31*(22), 3783-3795.

Millar, C., Pratt, D., Schneider, D. J., Koehler, G., & McDonnell, J. J. (2019). Further experiments comparing direct vapor equilibration and cryogenic vacuum distillation for plant water stable isotope analysis. *Rapid Communications in Mass Spectrometry*, *33*(23), 1850-1854.

Mitsch, W. J., Taylor, J. R., & Benson, K. B. (1991). Estimating primary productivity of forested wetland communities in different hydrologic landscapes. *Landscape Ecology*, *5*(2), 75-92.

Moerschbaecher, M. K., Keim, R. F., & Day, J. W. (2016). *Estimating carbon stocks in uneven-aged bottomland hardwood forest stands in south Louisiana.* In: Proceedings of the 18th biennial southern silvicultural research conference. e-Gen. Tech. Rep. SRS-212. Asheville, NC: US Department of Agriculture, Forest Service, Southern Research Station. 614 p.

Monteith, J. L. (1967). *Evaporation and Environment. The Stage and Movement of Water in Living Organisms*. In Forest Hydrology, edited by W.E. Sopper and H.W. Lull. Pergamon, Oxford, p 205-234.

Morales, S. R., Lemon, M. G. T., Stewart, R. D., & Keim, R. F. (2021). Flood-induced recharge of matrix water in a vertic forest soil. *Water Resources Research*, *57*(7), e2021WR029675.

National Cooperative Soil Survey. National Cooperative Soil Characterization Database. Available online. Accessed [April/2/2021].

NOAA National Centers for Environmental information, Climate at a Glance: County Time Series, published June 2021, retrieved on June 28, 2021a from https://www.ncdc.noaa.gov/cag/

NOAA National Centers for Environmental information, Local Climatological Data (LCD), published June 2021, retrieved on June 28, 2021b from https://www.ncdc.noaa.gov/cdo-web/datatools/lcd

O'Driscoll, M., DeWalle, D., McGuire, K., & Gburek, W. (2005). Seasonal 18O variations and groundwater recharge for three landscape types in central Pennsylvania, USA. *Journal of Hydrology*, *303*(1-4), 108-124.

Oerter, E., Finstad, K., Schaefer, J., Goldsmith, G. R., Dawson, T., & Amundson, R. (2014). Oxygen isotope fractionation effects in soil water via interaction with cations (Mg, Ca, K, Na) adsorbed to phyllosilicate clay minerals. *Journal of Hydrology*, *515*, 1-9.

Oerter, E. J., & Bowen, G. (2017). In situ monitoring of H and O stable isotopes in soil water reveals ecohydrologic dynamics in managed soil systems. *Ecohydrology*, *10*(4), e1841.

Or, D., Leij, F. J., Snyder, V., & Ghezzehei, T. A. (2000). Stochastic model for posttillage soil pore space evolution. *Water Resources Research*, *36*(7), 1641-1652.

Ozer, M., Orhan, M., & Isik, N. (2010). Effect of Particle Optical Properties on Size Distribution of Soils Obtained by Laser Diffraction. *Environmental & Engineering Geoscience - ENVIRON ENG GEOSCI*, *16*, 163-173.

Pataki, D., & Oren, R. (2003). Species differences in stomatal control of water loss at the canopy scale in a mature bottomland deciduous forest. *Advances in Water Resources*, *26*(12), 1267-1278.

Penna, D., Stenni, B., Šanda, M., Wrede, S., Bogaard, T., Michelini, M., . . . Zuecco, G. (2012). Evaluation of between-sample memory effects in the analysis of δ^2H and $\delta^{18}O$ of water samples measured by laser spectroscopes. *Hydrology and Earth System Sciences*, *16*(10), 3925-3933.

Philip, J., & De Vries, D. (1957). Moisture movement in porous materials under temperature gradients. *Eos, Transactions American Geophysical Union*, *38*(2), 222-232.

Pionke, H., & DeWalle, D. (1992). Intra-and inter-storm ^{18}O trends for selected rainstorms in Pennsylvania. *Journal of Hydrology*, *138*(1-2), 131-143.

Qiu, X., Zhang, M., Wang, S., Evaristo, J., Argiriou, A. A., Guo, R., . . . Qu, D. (2019). The test of the ecohydrological separation hypothesis in a dry zone of the northeastern Tibetan Plateau. *Ecohydrology*, *12*(3), e2077.

Radolinski, J., Pangle, L., Klaus, J., & Stewart, R. D. (2021). Testing the 'two water worlds' hypothesis under variable preferential flow conditions. *Hydrological Processes*, *35*(6), e14252.

Richards, L. A. (1931). Capillary conduction of liquids through porous mediums. *Physics*, *1*(5), 318-333.

Rodríguez-González, P. M., Stella, J. C., Campelo, F., Ferreira, M. T., & Albuquerque, A. (2010). Subsidy or stress? Tree structure and growth in wetland forests along a hydrological gradient in Southern Europe. *Forest Ecology and Management*, *259*(10), 2015-2025.

Rodriguez- Iturbe, I. (2000). Ecohydrology: A hydrologic perspective of climate- soil-vegetation dynamics. *Water Resources Research*, *36*(1), 3-9.

Rodriguez- Iturbe, I., D'Odorico, P., Laio, F., Ridolfi, L., & Tamea, S. (2007). Challenges in humid land ecohydrology: Interactions of water table and unsaturated zone with climate, soil, and vegetation. *Water Resources Research*, *43*(9).

Shockey, M. C., Stewart, R. D., Keim, R. F., (2021). Measuring shrinkage of undisturbed soil peds. *Soil Science Society of America Journal.* Manuscript submitted for publication.

Soil Survey Staff, Natural Resources Conservation Service, United States Department of Agriculture. Web Soil Survey. Available online at the following link: http://websoilsurvey.sc.egov.usda.gov/. Accessed [October/29/2019].

Sprenger, M., Llorens, P., Cayuela, C., Gallart, F., & Latron, J. (2019). Mechanisms of consistently disjunct soil water pools over (pore) space and time. *Hydrology and Earth System Sciences*, *23*(6), 2751-2762.

Sun, G., McNulty, S., Amatya, D., Skaggs, R., Swift Jr, L., Shepard, J., & Riekerk, H. (2002). A comparison of the watershed hydrology of coastal forested wetlands and the mountainous uplands in the Southern US. *Journal of Hydrology*, *263*(1-4), 92-104.

U.S. Army Corps of Engineers (2017). History of the Lower Mississippi Levee System.

Veihmeyer, F., & Hendrickson, A. (1955). Does transpiration decrease as the soil moisture decreases? *Eos, Transactions American Geophysical Union*, *36*(3), 425-448.

von Freyberg, J., Allen, S. T., Grossiord, C., & Dawson, T. E. (2020). Plant and root-zone water isotopes are difficult to measure, explain, and predict: Some practical recommendations for determining plant water sources. *Methods in Ecology and Evolution*, *11*(11), 1352-1367.

Wassenaar, L., Hendry, M., Chostner, V., & Lis, G. (2008). High resolution pore water $\delta^{2}H$ and $\delta^{18}O$ measurements by H_2O (liquid)− H_2O (vapor) equilibration laser spectroscopy. *Environmental science & technology, 42*(24), 9262-9267.

Weiler, M. & Flühler, H. (2004). Inferring flow types from dye patterns in macroporous soils. 767 *Geoderma*, *120*(1), 137–153. https://doi.org/10.1016/j.geoderma.2003.08.014

Wentworth, C. K. (1922). A scale of grade and class terms for clastic sediments. *The Journal of Geology*, *30*(5), 377-392.

Woessner, W. (2000). Stream and fluvial plain ground water interactions: rescaling hydrogeologic thought. *Ground Water*, *38*, 423-429.

Yue, K., De Frenne, P., Fornara, D. A., Van Meerbeek, K., Li, W., Peng, X., . . . Peñuelas, J. (2021). Global patterns and drivers of rainfall partitioning by trees and shrubs. *Global Change Biology*, *27*(14), 3350-3357.

Zhang, Y., Kong, D., Gan, R., Chiew, F. H. S., McVicar, T. R., Zhang, Q., & Yang, Y. (2019). Coupled estimation of 500 m and 8-day resolution global evapotranspiration and gross primary production in 2002–2017. *Remote Sensing of Environment*, *222*, 165-182.

VITA

Amanda Barbato grew up in south Florida. She received a Bachelor's of Science in Ocean and Coastal Resources with a minor in Geology from Texas A&M University at Galveston in December of 2018. Amanda attended Louisiana State University from 2019 to 2021, and plans to receive a Masters of Science in Renewable Natural Resources with a concentration in Watershed Hydrology this December. Following her graduation from Louisiana State University, she plans to continue working in ecohydrology as a Physical Scientist with the Environmental Protection Agency.